Protective effect of ginseng extract and total ginsenosides on hematopoietic stem cell damage by inhibiting cell apoptosis and regulating the intestinal microflora

ZUGUO LIANG[1,2*], XIANG GAO[1,2*], CHENXU JING[1], TONGYI YUAN[1,2], LANCAO ZHANG[3], YIFEI YIN[1,2], JIANZE OU[1,2], XIANGYAN LI[3], WENXIU QI[3], DAQING ZHAO[3], HANG SU[3] and HE ZHANG[1,2]

[1]Research Center of Traditional Chinese Medicine, The Affiliated Hospital to Changchun University of Chinese Medicine, Changchun, Jilin 130021, P.R. China; [2]College of Pharmacy, Changchun University of Chinese Medicine, Changchun, Jilin 130117, P.R. China; [3]Northeast Asia Research Institute of Traditional Chinese Medicine, Changchun University of Chinese Medicine, Changchun, Jilin 130117, P.R. China

Received April 19, 2024; Accepted October 7, 2024

DOI: 10.3892/ijmm.2024.5455

Abstract. Ginseng may improve the myelosuppression and intestinal microbiota disorder induced by cyclophosphamide (CY); however, the effect of ginseng components on hematopoietic stem cell (HSC) damage remains largely unexplored. The present study aimed to assess the protective effect of ginseng extract (GE), total ginsenosides (TG) and total polysaccharides (TP) from ginseng on the intestinal microflora and HSCs of model mice. In the present study, a mouse model of HSC damage induced by CY was constructed, intestinal microflora of fecal samples were sequenced using the 16S ribosomal RNA (rRNA) sequencing techniques, the differentially expressed genes (DEGs) of HSCs were analyzed using high-throughput RNA-sequencing, cell apoptosis and erythroid differentiation were detected using flow cytometry and the blood cell parameters were analyzed using a hematology analyzer. Analysis of the 16S rRNA in fecal samples showed that GE, TG and TP improved an imbalanced intestinal microflora, where the relative abundance of *Lactobacillus intestinalis* had a positive correlation with ginsenosides content. Specifically, TP significantly increased the expression of low-abundance microflora. Transcriptomic analysis results revealed 2,250, 3,432 and 261 DEGs in the GE, TG and TP groups compared with those in the Model group, respectively. In the expression analysis of DEGs, both TG and GE were found to markedly increase the expression levels of *Klf4*, *Hhex*, *Pbx1*, *Kmt2a*, *Mecom*, *Zc3h12a*, *Zbtb16*, *Lilr4b*, *Flt3* and *Klf13*. Furthermore, TG inhibited the apoptosis of HSCs by increasing the expression levels of *Bcl2* and *Mcl1*, whilst decreasing the expression of *Bax*. By contrast, GE inhibited the apoptosis of HSCs by reducing the expression of *Bax* and *Bad*. Regarding erythroid differentiation and blood cell parameters, GE was found to significantly increase the expression of TER-119. In addition, GE and TG improved all blood cell parameters, including the count of white blood cells, neutrophils (NEUT), lymphocytes (LYMPH), red blood cells (RBC), hemoglobin (HGB) and reticulocyte and platelets (PLT), whereas TP could only improve the counts of LYMPH, RBC, HGB and PLT. The improvement effect of GE and TG on WBC, NEUT and Ret was superior to TP. In conclusion, TG may protect the hematopoiesis function of HSCs in a CY-induced mouse model of HSC damage, followed by GE. However, TP did not appear to improve HSC damage. Ginsenosides may therefore be considered essential ingredients in GE when protecting HSCs against damage. GE and TG exerted their protective effects on HSCs by inhibiting the apoptosis of HSCs whilst improving the imbalance of intestinal microflora.

Correspondence to: Dr He Zhang, Research Center of Traditional Chinese Medicine, The Affiliated Hospital to Changchun University of Chinese Medicine, 1478 Gongnong Road, Changchun, Jilin 130021, P.R. China
E-mail: 13843148162@163.com

Dr Hang Su, Northeast Asia Research Institute of Traditional Chinese Medicine, Changchun University of Chinese Medicine, 1035 Boshuo Road, Changchun, Jilin 130117, P.R. China
E-mail: suhang0720@live.cn

*Contributed equally

Key words: ginseng extract, total ginsenosides, total polysaccharides, cyclophosphamide, hematopoietic stem cells, intestinal microflora, high-throughput RNA-sequencing

Introduction

Cyclophosphamide (CY) is an effective chemotherapeutic agent that can be used to treat various types of cancer (1-3), such as lymphoma, breast cancer and ovarian cancer. However, CY can also exert oxidative DNA damage on bone marrow cells, causing myelosuppression and immunosuppression (4). Notably, CY has been previously reported to trigger bone marrow cell apoptosis 6 h after administration (5). In addition, it can cause the hematopoietic inhibition of bone marrow and reduce the numbers of several peripheral blood cell types,

such as red blood cells (RBC), white blood cells (WBC) and platelets (PLT) (6). Furthermore, CY frequently causes intestinal mucositis and neutropenia, which result in intestinal microbiota disorder (7,8). Therefore, it is important to preserve the function of hematopoietic stem cells (HSCs) in the bone marrow during chemotherapy.

Ginseng (*Panax ginseng* C.A. Meyer) has been used to treat diseases for thousands of years in China. Modern pharmacological studies have previously shown that ginseng can treat various diseases, such as cancer, inflammation, oxidative stress, tumors, obesity and diabetes (9). The main chemical components contained within ginseng include ginsenosides, polysaccharides, phenolic acid and proteins (10). In the clinic, ginseng or ginsenosides have been frequently used to reduce the side effects induced by chemotherapy (5,11). Ginsenosides and polysaccharides are the important active ingredients of ginseng. The total ginsenosides (TG), ginsenoside Rb1, ginsenoside Rg1, ginsenoside compound K (CK) or ginsenoside Rh2 have been reported to possess dual effects, including anticancer and bone marrow-protecting activities (12,13). The ginseng polysaccharides have a number of pharmacological effects, such as anti-oxidative, anti-inflammatory, immunoregulatory and intestinal microbiota regulatory activities (14). It has previously been shown that ginseng polysaccharides can enhance the activity and absorption of ginsenosides by affecting intestinal microbial metabolism via increasing β-glucosidase activity (15).

Firmicutes (79.4%) and Bacteroidota (16.9%) constitute the main bacterial families in the intestines of healthy adult humans (16). Imbalance in the intestinal microflora can weaken the resistance of the body to pathogenic microorganisms, resulting in the loss of the protective intestinal barrier (17). *Lactobacillus*, *Streptococcus* and *Escherichia coli* can promote goblet cell differentiation and mucus production in the intestine to reduce the abundance of *Salmonella typhimurium* and pathogenic *Escherichia coli*, which preserves epithelial cell function and energy balance (18). By contrast, *Fusobacterium* have been reported to be enriched in patients with colon cancer, which can invade intestinal epithelial cells to enable their survival and maintenance, whereas the abundance of Bacteroidetes and Firmicutes are reduced in patients with colon cancer (19). Kostic *et al* (20) previously reported that *Fusobacterium* had a fitness advantage in the evolving tumor microenvironment, which caused an imbalance of gut microbiota. Notably, ginsenosides and ginseng polysaccharides have been shown to reverse gut microbiota disorder by inhibiting the expression of inflammatory cytokines, in turn restoring the diversity of intestinal microflora (21-23). Ginsenosides and polysaccharides from ginseng have shown protective effects on the imbalance of intestinal microflora (7).

Moreover, cell apoptosis induced by CY is the main cause of HSC damage (24), and ginsenosides protect HSCs from damage by reducing HSC apoptosis and inhibiting the expression of inflammation factors (25). Therefore, the present study assessed the effects of ginseng extract (GE), TG and total polysaccharides (TP) from ginseng on intestinal microflora regulation and the viability of bone marrow HSCs in a mouse model of HSC damage induced by CY via 16S ribosomal (r)RNA gene sequencing of fecal matter and the high-throughput RNA-sequencing of HSCs.

Materials and methods

Chemicals. CY (cat. no. S30563) was obtained from Shanghai Yuanye Biotechnology Co., Ltd. The cell apoptosis kit (Annexin V-FITC/PI; cat. no. 556547) was supplied by BD Pharmingen (BD Biosciences). Blood routine reagent kits (Staining reagent kit, cat. no. ZY4203 and Reaction reagent kit, cat. no. ZY4224) was purchased by IDEXX Laboratories Inc. The PE-conjugated anti-TER-119 antibody (cat. no. 116207) was obtained from BioLegend, Inc.

Preparation of GE, TG and TP. Dry *Panax ginseng* was purchased from the Wanliang ginseng market (Tonghua, China). The ginseng was boiled three times to obtain the GE (6). The extracting solution of GE was eluted with different concentrations of ethanol (80-95%), before being centrifuged at 1,200 x g at 4˚C for 20 min to obtain the supernatant and precipitates. The supernatant was sequentially decolorized with a decolorization resin (cat. no. D941; Tianjin Haoju Resin Technology Co., Ltd.) and activated carbon, before being filtered and dried at 40˚C to obtain TG (26). The precipitates were sequentially deproteinized, decolorized and dialyzed to remove components with a molecular weight of <3,500 Da to obtain the TP (27). The composition and content of ginsenosides and polysaccharides in the GE, TG and TP have been reported in a previous study (6,26). The ginsenoside content of GE and TG is 4.39 and 81.09%, respectively. By contrast, the polysaccharide content of GE, TG and TP is 72.28, 4.68 and 89.79%, respectively (26).

Animal model. A total of 50 male 4-week-old Kunming mice (weight, 18-20 g) were purchased from Liaoning Changsheng Biotechnology Co., Ltd. [animal license no. SCXK (Liao)-2015-0001]. The mice were maintained under the conditions of controlled light (12 h light/dark), temperature (25±1˚C) and humidity (60%±5%), with *ad libitum access* to food and water. After 5 days of acclimation, mice were randomly divided into the following five groups (n=10/group): i) The normal group (Control); ii) the group treated with CY (Model); iii) the CY + GE group (GE, 1.0 g/kg); iv) the CY + TG group (TG, 0.25 g/kg); and v) the CY + TP group (TP, 1.0 g/kg).

The mice were intragastrically administered GE, TG and TP for 28 days in the GE, TG and TP groups (0.1 ml/10 g body weight) (7,28), whereas mice in the other groups were administered equivalent volumes of normal saline. Mice in the Model, GE, TG and TP groups were hypodermically injected with CY saline solution (50 mg/kg) on days 25, 26, 27 and 28. The dose of GE was calculated according to the human adult daily dose of ginseng (9 g/day, 60 kg/body weight) (29), whereas the doses of TG and TP (1.0 g/kg) were selected according to previous studies (6,7).

The fresh feces of mice were collected on day 28 and stored at -80˚C until further analysis. All mice were then euthanized by cervical dislocation under anesthesia with 30 mg/kg pentobarbital sodium by intraperitoneal injection after fasting for 12 h. If an animal reached the predefined humane endpoints [loss of >15% of body weight in 1-2 days or an overall reduction of >20% in body weight; or displaying obvious signs of suffering (lethargy, squinted eyes, dehydration and hunched

back)], they were humanely euthanized as aforementioned. Animal death was confirmed by cessation of respiration and heartbeat. The study protocol was approved by the Ethics Committee of Changchun University of Chinese Medicine (protocol no. 2023033; Changchun, China). No mice showed abnormal signs or reached humane endpoints throughout the experiment.

Blood cell parameters. Anesthesia with 30 mg/kg pentobarbital sodium (concentration 5 mg/ml, dose 60 μl/10 mg body weight) was induced by intraperitoneal injection on day 29. Subsequently, ~0.5 ml blood was collected from the retro-orbital vein (30). The mice were then sacrificed after this blood collection. The blood cell parameters [WBC, neutrophils, lymphocytes (LYMPH), RBC, hemoglobin (HGB), reticulocytes (Ret) and PLT] were detected using the ProCyte DX hematology analyzer (IDEXX Laboratories Inc.).

16S rRNA gene sequencing. A QIAamp DNA Stool Mini Kit (cat. no. 51504; Qiagen, Inc.) was used to extract and purify the DNA of the fecal samples (7 samples from 7 mice each group). The primers (341F: 5'-CCTAYGGGRBGCASCAG-3' and 806R: 5'-GGACTACNNGGGTATCTAAT-3') were used to amplify the 16S rRNA genes in the V3-V4 region. The library construction (NEBNext® Ultra™ IIDNA Library Prep Kit; cat. no. E7645; New England BioLabs, Inc.) and RNA sequencing were performed by Novogene Bioinformatics Technology Co., Ltd. The detailed steps of this sequencing procedure have been previously reported (6,31). For the effective tags obtained previously, denoise was performed with DADA2 or deblurmodule in the QIIME2 software (version QIIME2-202006; https://library.qiime2.org) to obtain initial amplicon sequence variants (ASVs; default: DADA2), and then ASVs with abundance <5 were filtered out. the annotation database was the Silva Database (https://www.arb-silva.de/). The following analyses were performed: i) Principal co-ordinates analysis was performed according to the weighted UniFrac distance matrices; ii) α-diversity was calculated from 4 indexes in QIIME2, including Chao1, Dominance, Pielou_e, and Shannon; iii) cluster analysis was performed with principal component analysis (PCA), which was applied to reduce the dimension of the original variables using the ade4 package and ggplot2 package in R software (version 3.5.3); iv) the significantly different species ($P<0.05$) at each taxonomic level (phylum, class, order, family, genus and species) were analyzed using the R software (version 3.5.3), $P<0.05$ was considered to indicate a statistically significant difference; and v) the LEfSe software (version 1.0) was used to perform LEfSe analysis] linear discriminant analysis (LDA) score >3; Kruskal-Wallis test, false discovery rate $P<0.05$] so as to identify the biomarkers.

Apoptosis of HSCs. Bone marrow from the right femur of the mice in the Control, Model, GE, TG and TP groups (n=10/group) was washed with PBS into the EasySep™ buffer (cat. no. 20144; Stemcell Technologies, Inc.) at room temperature using a syringe equipped with a 23-gauge needle to maintain the viability of bone marrow cells. The remaining aggregates and debris were removed by passing the cell suspension through a 70-μm mesh nylon strainer, before the sample was centrifuged at 300 x g for 10 min at room temperature. The cells were then resuspended at $1x10^8$ nucleated cells/ml in DMEM/F12 (cat. no. 11-330-032; Gibco; Thermo Fisher Scientific, Inc.). The HSCs from bone marrow mononuclear cells were purified using the EasySep™ Mouse Hematopoietic Progenitor Cell Isolation Kit according to manufacturer's protocol (cat. no. 19856; Stemcell Technologies, Inc.). HSCs were adjusted to $1x10^5$ cells/ml in PBS and were then labeled using Annexin V-FITC/PI (cat. no. c1052) for 20 min at room temperature. A total of 10,000 events were acquired to analyze cell apoptosis using a DxFLEX flow cytometer and CytExpert Software version 2.4.0.28 (both Beckman Coulter, Inc.).

Erythroid differentiation of HSCs. HSCs ($1x10^5$) were incubated with the PE-conjugated anti-TER-119 antibody (1:1,000) in the dark for 40 min on ice. Subsequently, TER-119 expression was detected using a DxFLEX flow cytometer and CytExpert software version 2.4.0.28 (both Beckman Coulter, Inc.).

RNA extraction, establishment of cDNA library and sequencing. Total RNA was extracted from HSCs according to the instruction manual of the TRIzol reagent (cat. no. AM9738; Thermo Fisher Scientific, Inc.). RNA concentration and purity was measured using a NanoDrop 2000 (Thermo Fisher Scientific, Inc.). RNA integrity was assessed using the RNA Nano 6000 Assay Kit (cat. no. 5067-1511) of the Agilent Bioanalyzer 2100 system (both Agilent Technologies, Inc.). A total of 1 μg RNA per sample was used as input material for the RNA sample preparations. Sequencing libraries were generated using NEBNext UltraTM RNA Library Prep Kit (cat. no. E7530S/L; New England BioLabs, Inc.) for Illumina following the manufacturer's recommendations. To select cDNA fragments preferentially of 240 bp in length, the library fragments were purified with AMPure XP system (Beckman Coulter, Inc.). Then, 3 μl USER Enzyme (cat. no. E7530S/L; New England BioLabs, Inc.) was used with size-selected, adaptor-ligated cDNA at 37˚C for 15 min followed by 5 min at 95˚C before PCR. PCR was then performed using Phusion High-Fidelity DNA polymerase (cat. no. M0530S; New England BioLabs, Inc.) with the following reaction conditions: 98˚C for 30 sec; 25 cycles of 98˚C for 10 sec and 72˚C for 15 sec; 72˚C for 5 min, 4˚C for hold. At last, the PCR products were purified (AMPure XP system) and the library quality was assessed on the Agilent Bioanalyzer 2100 system. The loading concentration of the final library was 2 nM. The clustering of the index-coded samples was performed on a cBot Cluster Generation System using TruSeq PE Cluster Kit v4-cBot-HS (Illumina) according to the manufacturer's instructions. After cluster generation, the library preparations were sequenced on an Illumina platform and paired-end reads were generated. The libraries were constructed and sequenced by Beijing Biomarker Technologies Co., Ltd. (www.biocloud.net).

Differentially expressed gene (DEG) analysis. After sequencing, bioinformatics analysis was performed using BMKCloud (www.biocloud.net) to identify the DEGs. Differential expression analysis of two conditions/groups was performed using DESeq2 (version 1.30.1; https://www.bioconductor.org/packages/release/bioc/html/DESeq2.html). An adjusted $P<0.05$ and a fold change (FC) of >1.5 were

considered to indicate a significant difference. Gene Ontology (GO) enrichment analysis of DEGs was implemented by the GOseq R packages-based Wallenius non-central hyper-geometric distribution (32). KOBAS software (33) was used to test the statistical enrichment of differential expression genes in Kyoto Encyclopedia of Genes and Genomes (KEGG) pathways (http://www.genome.jp/kegg/). Heatmap analysis of DEGs was conducted according to the FPKM value using the cluster Profiler package (version 3.0.3) in the R software.

Reverse transcription-quantitative PCR (RT-qPCR). Total RNA was extracted from HSCs using TRIzol® reagent (Invitrogen; Thermo Fisher Scientific, Inc.) and cDNA was obtained using the FastKing RT Kit (Tiangen Biotech Co., Ltd.) according to the manufacturer's protocol. Subsequently, qPCR was performed using the CFX Connect Real-Time PCR Detection System (Bio-Rad Laboratories, Inc.) with SuperReal PreMix Plus (SYBR Green; Tiangen Biotech Co., Ltd.). The primer sequences were as follows: *β-actin* forward, 5'-CTG TCCCTGTATGCCTCTG-3' and reverse, 5'-ATGTCACGC ACGATTTCC-3'; *Hhex* forward, 5'-CCACCCGAGAGAAAG CGTCTG-3' and reverse, 5'-TGCGTTGGACAGTTTGGA CACT-3'; *Klf4* forward, 5'-GCGGGAAGGGAGAAGACA CTGCGTC-3' and reverse, 5'-TAGGAGGGCCGGGTTGTT ACTGCT-3'; *Pira2* forward, 5'-ACTACTGGACACCCAGCC TT-3' and reverse, 5'-TGAACCTGTCATAGCTCGGC-3'; and *Pbx1* forward, 5'-TGAAGCCTGCCTTGTTTAATGT-3' and reverse, 5'-ATGTTGTCCAGTCGCATGAGC-3'. The thermocycling conditions were as follows: 95˚C for 15 min, followed by 40 cycles at 95˚C for 10 sec, 55˚C for 20 sec and 72˚C for 30 sec. The transcript levels were quantified and normalized to the internal reference gene *β-actin* using the $2^{-\Delta\Delta Cq}$ method (34).

Immunohistochemical analysis. The bone marrow from the left femurs of mice in the Control, Model, GE, TG and TP groups (n=6/group) was fixed in 10% formalin solution for 5 days at room temperature and demineralized with 10% EDTA for 14 days at room temperature. The samples were then embedded in paraffin and sectioned into 4 μm slices. Bone marrow tissue sections were dewaxed and then treated with high-pressured 2% EDTA (pH 9.0) antigen retrieval buffer at 95˚C for 20 min for antigen retrieval. The tissue was incubated in Endogenous Peroxidase Blocking Buffer (cat. no. P0100A; Beyotime Institute of Biotechnology) at room temperature for 10 min to block and eliminate the interference of endogenous peroxidase. Subsequently, the sections were blocked with 3% BSA (cat. no. B24726; Shanghai Angyi Biotechnology Co., Ltd.) for 1 h at room temperature, and then incubated with primary antibodies overnight at 4˚C. The sections were then incubated with secondary antibody [goat anti-rabbit IgG (H+L); cat. no. SA00001-2; Proteintech Group, Inc.; diluted to 1:1,000 in 3% BSA] at room temperature for 30 min. Finally, the binding antibody was detected by DAB (cat. no. DAB-2031; Fuzhou Maixin Biotechnology Development Co., Ltd.) staining at room temperature for 5 min and hematoxylin counterstaining at room temperature for 2 min. Negative (no primary antibody) control staining of one mouse was used in each experiment. Images were captured using the Axioscan 7 fully automatic digital slide scanning system (Zeiss AG). Rabbit anti-mouse Klf4 (cat. no. 11880-1-AP; Proteintech Group, Inc.) and rabbit anti-mouse Pbx1 (cat. no. 18204-1-AP; Proteintech Group, Inc.) antibodies were used as primary antibodies to detect protein expression in PBS-Tween (1%) at a concentration of 1:200.

Western blot analysis. Western blot analysis was performed as previously reported (35). Briefly, the proteins were extracted from the bone marrow cells of mice tibia and femur, and then lysed in RIPA lysis buffer (cat. no. P0013B; Beyotime Institute of Biotechnology) containing protease inhibitors (cat. no. 05892970001; Roche Diagnostics) at 4˚C for 5 min. Subsequently, 35 μg protein was separated by 12% SDS-PAGE and then transferred onto PVDF membranes. The membranes were blocked with 3% BSA for 1 h at room temperature, and then incubated with the following primary antibodies (all from Proteintech Group, Inc.) overnight at 4˚C: β-actin (1:2,000; cat. no. BS6007M), Bcl2 (1:2,000; cat. no. 26593-1-AP) and Bax (1:2,000; cat. no. 50599-2-Ig). The membranes were then incubated with a secondary antibody [goat anti-rabbit IgG (H+L) 1:5,000; cat. no. SA00001-2; Proteintech Group, Inc.] for 2 h at room temperature. The bands were visualized using an ECL luminescence reagent (cat. no. P001-500; Hunan Hui Bai Shi Biological Technology Co., Ltd.) a ChemiDoc™ MP imaging system (Bio-Rad Laboratories, Inc.) at room temperature. The relative protein expression levels were normalized to β-actin.

Statistical analysis. The DEGs were filtered according to fold change ≥1.5 and $P<0.05$. Quantitative data are presented as the mean ± SD. The relative abundance of intestinal microflora was compared between groups using one-way ANOVA followed by Dunnett's test, whereas other data were analyzed with one-way ANOVA followed by Tukey's test using GraphPad Prism 8.0 software (Dotmatics). Correlation analysis was performed using Spearman's rank correlation coefficient test. $P<0.05$ was considered to indicate a statistically significant difference.

Results

Statistical analysis of α diversity in intestinal microflora. Fig. 1A shows the number of shared and unique ASVs among the five treatment groups in a Venn diagram. There were 343, 741, 469, 539 and 624 unique ASVs in the Control, Model, GE, TG and TP groups, respectively. The principal co-ordinates analysis showed that the microbial community had some differences between the Control and Model or TP groups (Fig. 1B). The α diversity reflects the richness and evenness of intestinal microflora. The Chao 1 index shows the community richness, which is positively associated with the number of ASVs. The dominance index and pielou_e index show the community evenness, whilst the Shannon index shows the richness and evenness of ASVs. As shown in Fig. 1C, CY markedly decreased the Chao 1 index compared with that in the Control group. In addition, GE, TG and TP increased the Chao 1, pielou_e and Shannon indices, whilst reducing the dominance index compared with the Model group; however, these differences were not statistically significant. These results indicated that GE, TG and TP markedly increased the community richness and evenness of ASVs in model mice. Notably, 7 samples from 7 mice in the TP group showed the best uniformity (Fig. 1B and C).

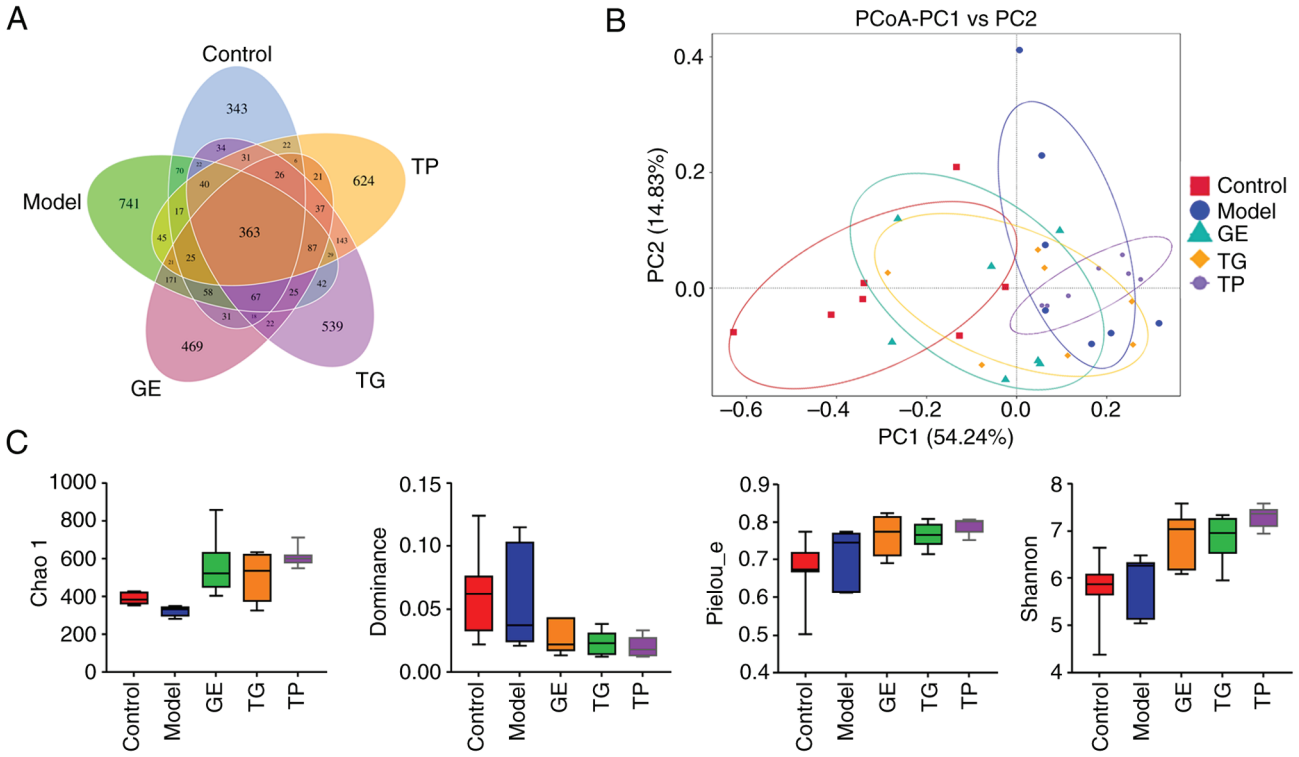

Figure 1. Statistical analysis of αin intestinal microflora. (A) Venn diagram of overlapping amplicon sequence variants among the five treatment groups. (B) Principal co-ordinates analysis. (C) α-diversity included Chao 1, Dominance, Pielou_e and Shannon indexes. PCoA, principal components analysis; PC, principle component; GE, ginseng extract; TG, total ginsenosides; TP, total polysaccharides.

Differences in the relative abundance of bacteria phylum, genus and species. The present study next analyzed the composition and abundance of the top 10, 15 and 15 bacteria at the phylum, genus and species levels, respectively. CY increased the relative abundance of Bacteroidota whilst decreasing that of Firmicutes at the phylum level (Fig. 2A). GE was found to significantly elevate the abundance of Firmicutes compared with that in the Model group (Fig. 2B). TG and TP also increased the expression of Firmicutes, whereas GE and TG also reduced the abundance of Bacteroidota. However, the difference was not statistically significant (Fig. 2B). Fig. 2C and D show the top 15 genera at the genus level clustered according to the relative abundance among the five groups (n=35 samples). CY significantly reduced the relative abundance of *Lactobacillus*, whilst increasing that of *Bacteroides*, *Alloprevotella* and *Muribaculaceae* (Fig. 2E). GE significantly increased the relative abundance of *Lactobacillus*. By contrast, TG also increased the relative abundance of *Lactobacillus* compared with that in the Model group, but the difference was not significant (Fig. 2E). In addition, GE and TG were found to reduce the relative abundance of *Clostridia_UCG-014* and *Odoribacter* compared with the Model group (Fig. 2E). These results suggest that GE at least partially reversed the abnormal changes in some intestinal microflora, followed by TG and TP.

At the species level, CY increased the relative abundance of *Bacteroides_sartorii*, *Candidatus_arthromitus*, *Bacteroides_vulgatus* and *Mucisporollum*_sp., whilst decreasing that of *Lactobacillus_intestinalis* and *Metamycoplasma_sualvi* (Fig. 2F). GE, TG and TP could reverse these aforementioned changes in the intestinal microflora. Notably, GE and TG significantly increased the abundance of *Lactobacillus_intestinalis* compared with that in model group (Fig. 2G). In addition, *Lactobacillus_intestinalis* was significantly positively correlated with ginsenoside content (r=0.8705; Fig. 2H). Furthermore, TP increased the abundance of low-abundance microflora compared with the Control group, such as *Mouse_gut*, *Bacteroides_dorei*, *Prevotella_melanimogenica*, *Anaerotignum_lactatifermentans*, *Bacteroides_plebeius* and *Parabacteroides_merdae*. Although CY and TP increased the abundance of some low-abundance microflora, the bacterial species were different. These results showed that the intestinal bacteria of model mice treated with GE, TG and TP were markedly improved. In general, the relative abundance and species of intestinal bacteria recovered by GE were consistent with the Control group at the phylum, genus and species levels.

The key microflora (biomarkers) were next identified using LDA (Fig. 3A) and an evolutionary branch tree (Fig. 3B). A total of 4, 9 and 48 key microflora (LDA score >3) were detected in the GE, TG and TP groups, respectively (Fig. 3A). *s_Vibrio_metschnikovii*, *s_Streptococcus_hyointestinalis*, *s_Clostridium_fusiformis* and *s_Eubacterium_plexicaudatum* were key species in the GE group. The key species in the TG group included *f_Prevotellaceae*, *s_Lactobacillus_intestinalis*, *g_Alloprevotella* and o_Burkholderiales. By contrast, c_, p_ and o_Bacteroidales, *f_Muribaculaceae* and *g_Muribaculaceae* were higher in the TP group compared with that in the other groups.

Profiling of DEGs from HSCs using high-throughput RNA-seq analysis. A total of 27,684 genes were annotated and used for further analysis. There were 4,988 DEGs in all samples. PCA

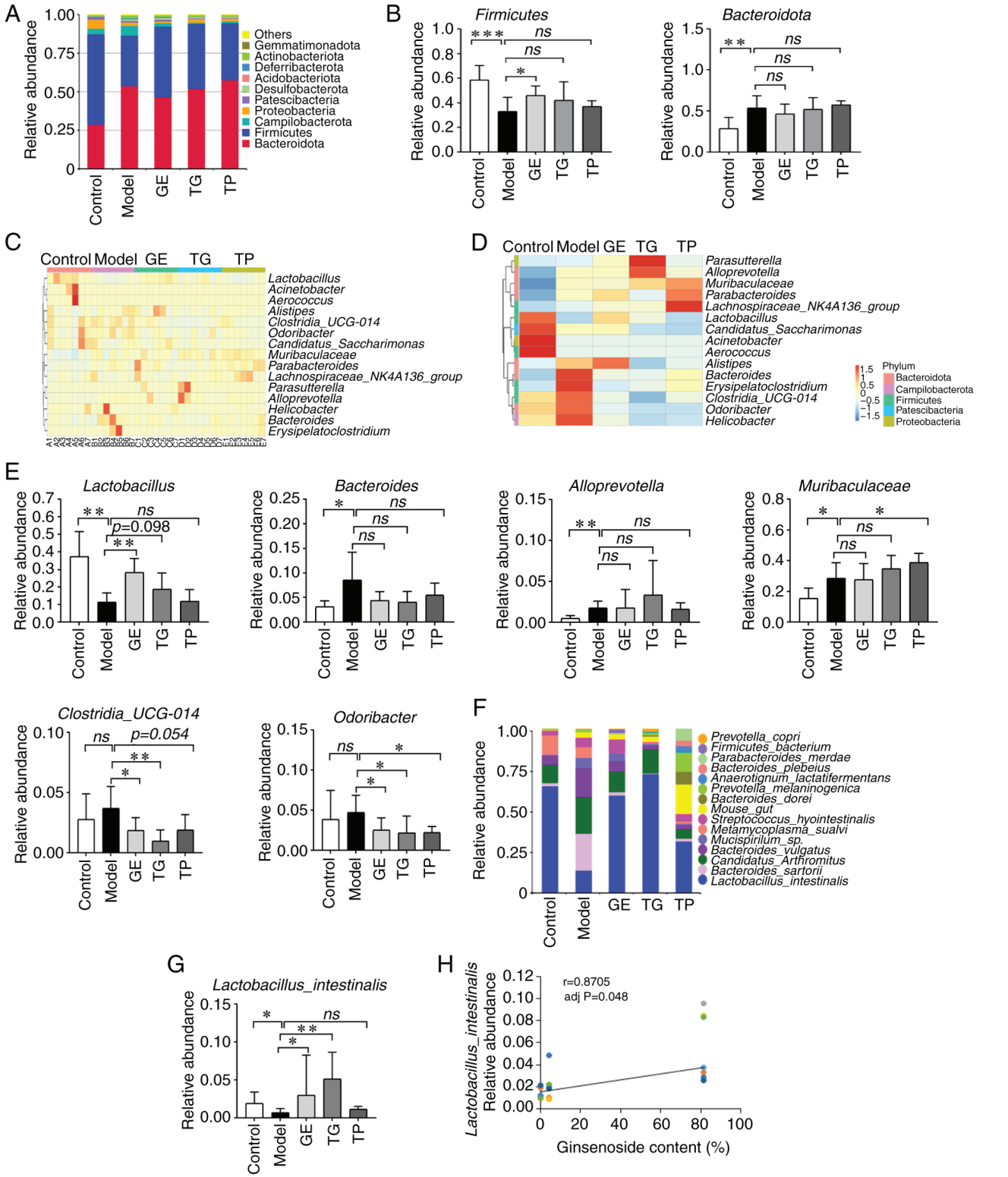

Figure 2. Analysis of the relative abundance in mice intestinal microflora among the GE, TG and TP groups. (A) Relative abundance of the top 10 bacteria at the phylum level. (B) Analysis of intestinal microflora among the treatment groups at the phylum level. (C) Heatmap of relative abundance of the top 15 genera among the 35 samples at the genus level. (D) Heatmap of relative abundance of the top 15 genera among the five groups at the genus level. (E) Analysis of intestinal microflora among the groups at the genus level. (F) Relative abundances of the top 15 bacteria at the species level. (G) Relative abundances of *Lactobacillus_intestinalis* at the species level. (H) Spearman's correlation analysis between *Lactobacillus_intestinalis* and ginsenoside content. Data are presented as the mean ± SD (n=7). *P<0.05, **P<0.01 and ***P<0.001 vs. Model group. adj, adjusted; GE, ginseng extract; ns, no significance; TG, total ginsenosides; TP, total polysaccharides.

showed marked differences between the Model/TP group and GE/TG groups (Fig. 4A). Fig. 4B shows that a total of 1,746 DEGs were obtained between the Model and Control groups, with 716 upregulated and 1,030 downregulated. There were 2,250 DEGs between the Model and GE groups, including 1,258 upregulated and 992 downregulated DEGs. The highest

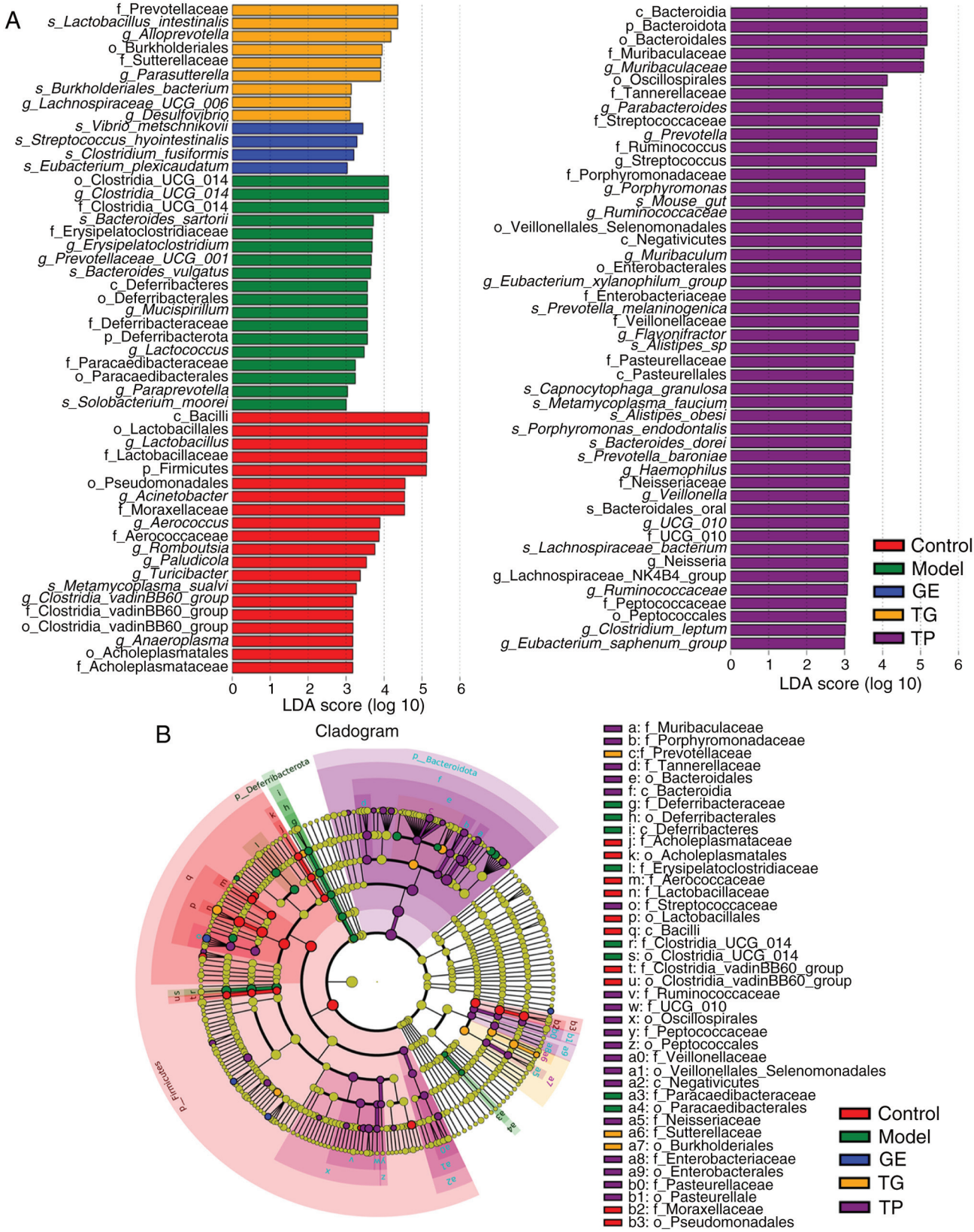

Figure 3. Linear discriminant analysis effect size difference analysis of the relative abundance of intestinal microflora among the GE, TG and TP groups. (A) LDA scores. (B) Evolutionary branch diagram. (n=7). c, class; f, family; g, genus; GE, ginseng extract; k, kingdom; LDA, linear discriminative analysis; o, order; p, phylum; s, species; TG, total ginsenosides; TP, total polysaccharides.

number of DEGs was detected between the Model and TG groups, including 1,833 upregulated DEGs and 1,599 downregulated DEGs. The lowest number of DEGs was detected between the Model and TP groups, including 75 upregulated DEGs and 186 downregulated DEGs. A Venn diagram shows the numbers of upregulated DEGs (Fig. 4C) and

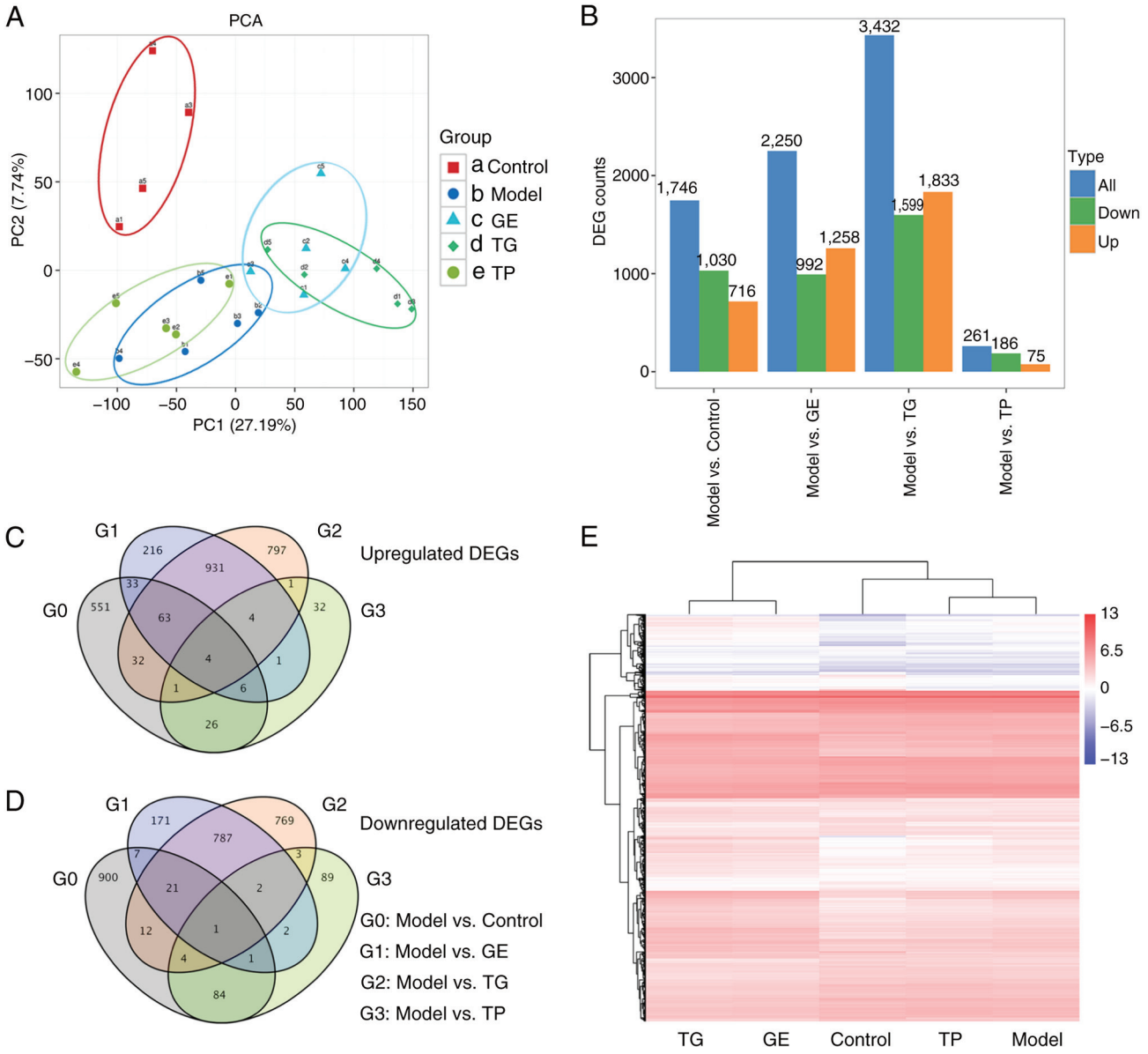

Figure 4. Profiling of DEGs (fold change ≥1.5; P<0.01) from hematopoietic stem cells among the treatment groups. (A) PCA of genes among the groups. (B) Counts of DEGs between the various indicated two treatment groups. Venn diagrams of (C) upregulated and (D) downregulated DEGs among groups. (E) Heatmap of DEGs among groups. DEGs, differentially expressed genes; GE, ginseng extract; PCA, principal component analysis; TG, total ginsenosides; TP, total polysaccharides.

downregulated DEGs (Fig. 4D) among the groups. There were 4 upregulated DEGs and 1 downregulated DEG in common between the Model and Control/GE/TG/TP (Fig. 4C and D). Cluster analysis was performed for the five groups based on 4,988 DEGs, where the profiling of the DEGs was found to be similar between the TG and GE groups or between the Model and TP groups (Fig. 4E).

GO analysis of the upregulated DEGs from HSCs. In the top 20 biological processes, upregulated genes in the Control group compared with the Model group (Fig. 5A) were mainly enriched in immune regulation (including 'immune response', 'neutrophil chemotaxis', 'myeloid leukocyte differentiation', 'acute inflammatory response' and 'B cell proliferation involved in immune response') and hemopoiesis regulation (including 'negative regulation of cell proliferation', 'response to hypoxia', 'hemopoiesis', 'positive regulation of nitric oxide biosynthetic process', 'cellular response to decreased oxygen levels', 'cellular response to oxygen levels' and 'cellular response to macrophage colony-stimulating factor stimulus'). In the top 20 biological processes, the upregulated genes in the GE group compared with the Model group (Fig. 5B) were enriched in immune regulation ('transforming growth factor beta receptor signaling pathway' and 'negative regulation of interleukin-6 production') and hemopoiesis regulation ('small GTPase mediated signal transduction', 'positive regulation of blood vessel endothelial cell migration', 'regulation of small GTPase mediated signal transduction', 'cellular response to vascular endothelial growth factor stimulus' and 'positive regulation of nitric-oxide synthase biosynthetic process'). Compared with the Model group, the upregulated genes in the TG group (Fig. 5C) were related to 'inflammatory response', 'small

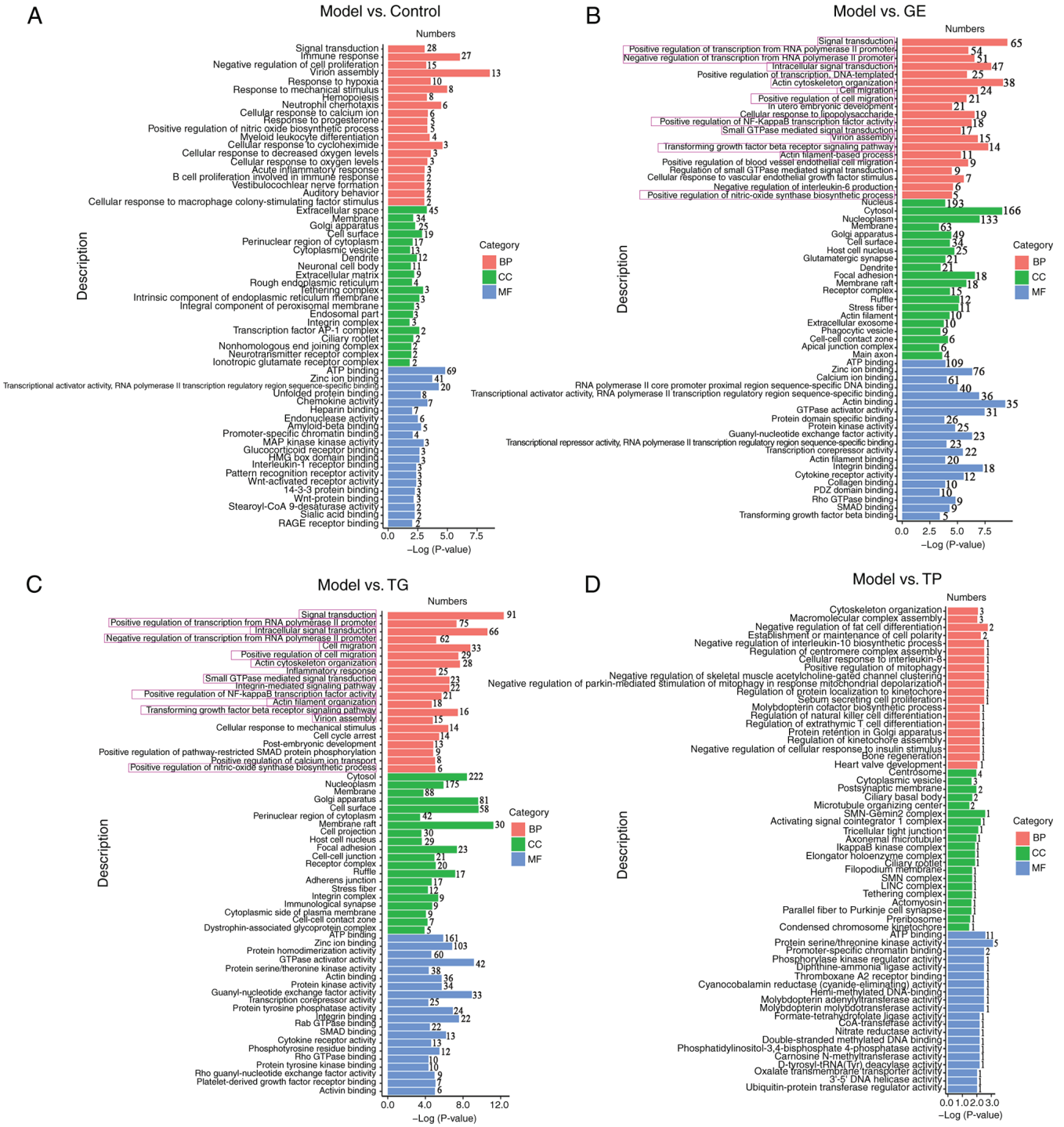

Figure 5. Top 20 GO terms associated with the upregulated DEGs in hematopoietic stem cells between the various indicated two treatment groups. Top 20 GO terms associated with the DEGs between the (A) Model and Control groups, (B) Model and GE groups, (C) Model and TG groups and (D) Model and TP groups. BP, biological processes; CC, cellular components; DEGs, differentially expressed genes; GE, ginseng extract; GO, Gene Ontology; MF, molecular functions; TG, total ginsenosides; TP, total polysaccharides.

GTPase mediated-signal transduction' and 'positive regulation of nitric-oxide synthase biosynthetic process' in the top 20 biological processes. Compared with the Model group, the upregulated genes in the TP group (Fig. 5D) were enriched in immune regulation ('negative regulation of interleukin-10 biosynthetic process', 'cellular response to interleukin-8', 'regulation of natural killer cell differentiation' and 'regulation of extrathymic T cell differentiation') and 'negative regulation of parkin-mediated stimulation of mitophagy in response to mitochondrial depolarization' terms. These results suggest that CY mainly affected the immune regulation and hematopoietic function of HSCs. In addition, the upregulated genes in the GE and TG groups showed similar enrichment results regarding biological processes (Fig. 5B and C, pink rectangles).

In the cellular component analysis, compared with the Model group, the upregulated genes in the GE and TG groups were mainly enriched in the 'cytosol', 'nucleoplasm', 'membrane', 'Golgi apparatus' and 'cell surface' (Fig. 5B and C), where

the upregulated genes in the GE group were also enriched in the 'nucleus'. By contrast, the upregulated genes in the TP group were primarily related to the 'centrosome', 'cytoplasmic vesicle' and 'postsynaptic membrane' compared with the Model group (Fig. 5D). The main cellular component enriched by TP were different from GE and TG.

In the molecular function analysis, the upregulated genes in the Control, GE, TG and TP groups were mainly enriched in 'ATP binding' (Fig. 5A-C). In particular, the upregulated DEGs in the GE and TG groups were also enriched in 'zinc ion binding,' 'GTPase activator activity', 'actin binding', 'protein kinase activity', 'guanyl-nucleotide exchange factor activity', 'transcription corepressor activity', 'integrin binding', 'SMAD binding', 'cytokine receptor activity' and 'Rho GTPase binding' (Fig. 5B and C). However, TP showed obvious differences compared with the Control, GE and TG groups regarding molecular function. The upregulated genes in the TP group were mainly enriched in 'protein serine/threonine kinase activity', 'promoter-specific chromatin binding' and 'phosphorylase kinase regulator activity' (Fig. 5D). The majority of the genes enriched in the GE and TG groups were consistent in the top 20 GO analysis.

KEGG analysis of the upregulated DEGs from HSCs. A total of 4,988 DEGs were involved in 297, 282, 306 and 125 KEGG pathways in the Control, GE, TG and TP groups, respectively. The DEGs were divided mainly into four branches based on KEGG annotations: Cellular processes, environmental information processing, human diseases and organismal systems. In cellular processes, the upregulated DEGs were enriched in 'endocytosis' and 'apoptosis' pathways in the Control, GE, TG and TP groups (Fig. 6A-D). Furthermore, 20 and 37 DEGs were enriched in 'signaling pathways regulating pluripotency of stem cells' in the GE and TG groups (Fig. 6B and C). In environmental information processing, the DEGs in the GE and TG groups were enriched mainly in the 'MAPK signaling pathway', 'PI3K-Akt signaling pathway', 'Rap1 signaling pathway', 'cytokine-cytokine receptor interaction', 'Ras signaling pathway', 'Wnt signaling pathway', 'apelin signaling pathway', 'JAK-STAT signaling pathway' and 'NF-kappa B signaling pathway'. The majority of these pathways are involved in the regulation and differentiation of HSCs (Fig. 6B and C) (36,37). The DEGs in the TP group were also mainly enriched in the 'MAPK signaling pathway', 'NF-kappa B signaling pathway', 'Rap1 signaling pathway', 'Wnt signaling pathway', 'apelin signaling pathway' and 'cell adhesion molecules'. In organismal systems, the DEGs were involved in 'osteoclast differentiation', 'Chemokine signaling pathway', 'C-type lectin receptor signaling pathway' and 'NOD-like receptor signaling pathway' in the Control, GE, and TG groups (Fig. 6A-C). TP exhibited notable differences compared with the GE and TG groups regarding organismal systems, where the DEGs were enriched in 'parathyroid hormone synthesis, secretion and action' and 'aldosterone synthesis and secretion' (Fig. 6D). The DEGs from the GE and TG groups participated mainly in regulating HSCs-related signaling pathways, such as 'MAPK signaling pathway', 'PI3K-Akt signaling pathway', 'Rap1 signaling pathway', 'cytokine-cytokine receptor interaction', 'Ras signaling pathway', 'Wnt signaling pathway', 'JAK-STAT signaling pathway' and 'NF-kappa B signaling pathway'. In addition, TP modulated HSCs-related signaling pathways. However, there were clear differences between the GE/TG and TP groups in terms of the profile of DEGs.

Expression analysis of the hematopoietic-related genes of the upregulated DEGs from HSCs. According to the GO analysis, the hematopoietic-related term of the upregulated DEGs had 'hemopoiesis', 'embryonic hemopoiesis', 'post-embryonic hemopoiesis', 'definitive hemopoiesis', 'regulation of hemopoiesis', 'negative regulation of hemopoiesis' and 'positive regulation of hemopoiesis'. Compared with the Model group, 9, 19, 23 and 1 DEGs were enriched in hematopoietic-related term in the Control, GE, TG and TP groups, respectively (Table SI). A total of 35 upregulated hematopoietic-related genes were clustered according to FPKM (Fig. 7A; Table SI). As shown in Fig. 7B, CY markedly decreased the expression levels of *Klf4*, *Hhex* and *Pira2*, whilst increasing those of *Flt3* and *Klf13*, compared with those in the Control group. These results indicated that CY affected HSCs. GE and TG significantly increased *Klf4* and *Hhex* expression compared with that in the Model group, whereas the expression levels of *Hhex* and *Klf4* were higher in the GE group compared with those in the TP group (Fig. 7B). The expression levels of *Pbx1*, *Kmt2a*, *Mecom*, *Zc3h12a*, *Zbtb16*, *Lilr4b*, *Flt3* and *Klf13* were higher in the GE and TG groups than those in the Model and TP groups (Fig. 7B). In addition, TG markedly increased the expression of *Pira2* compared with that in the Model, GE and TP groups (Fig. 7B). *Vpreb1* expression in the Control and TG groups was higher compared with that in the Model group, but the difference was not statistically significant (Fig. 7B). These results suggest that both TG and GE activated the expression of hematopoietic-related genes, though TP conferred almost no activating effect on the HSCs.

The mRNA expression levels of several genes were next detected in HSCs. As shown in Fig. 7C, CY markedly decreased the expression levels of *Klf4*, *Hhex*, *Pira2* and *Pbx1*. In the drug administration groups, GE significantly upregulated the expression levels of *Klf4*, *Hhex* and *Pbx1* compared with those in the Model and TP groups (Fig. 7C). TG also increased *Klf4*, *Hhex* and *Pira2* expression compared with that in the Model and TP groups (Fig. 7C). The expression of *Pbx1* in HSCs treated with TG was also significantly higher compared with that in the Model group (Fig. 7C). TP only significantly increased the expression of *Hhex* compared with the Model group (Fig. 7C). Other genes measured in the TP group exhibited slightly higher expression compared with those in the Model group, but no statistical significance could be found. In addition, the protein expression levels of Klf4 and Pbx1 were detected by immunohistochemistry. As shown in Fig. 8A and B, positive Klf4 and Pbx1 protein expression was markedly increased in the TG and GE groups compared with that in the Model group. The aforementioned results appeared to be consistent with the results of RNA-seq analysis.

Effect of GE, TG and TP on the apoptosis of HSCs. CY was found to promote the apoptosis of HSCs at the early and late apoptosis stages, whereas GE, TG and TP could inhibit the early apoptosis, late apoptosis and total apoptosis of HSCs induced by CY (Fig. 9A). TG exhibited the strongest effect on inhibiting cell apoptosis, whereas the effect of TG and GE

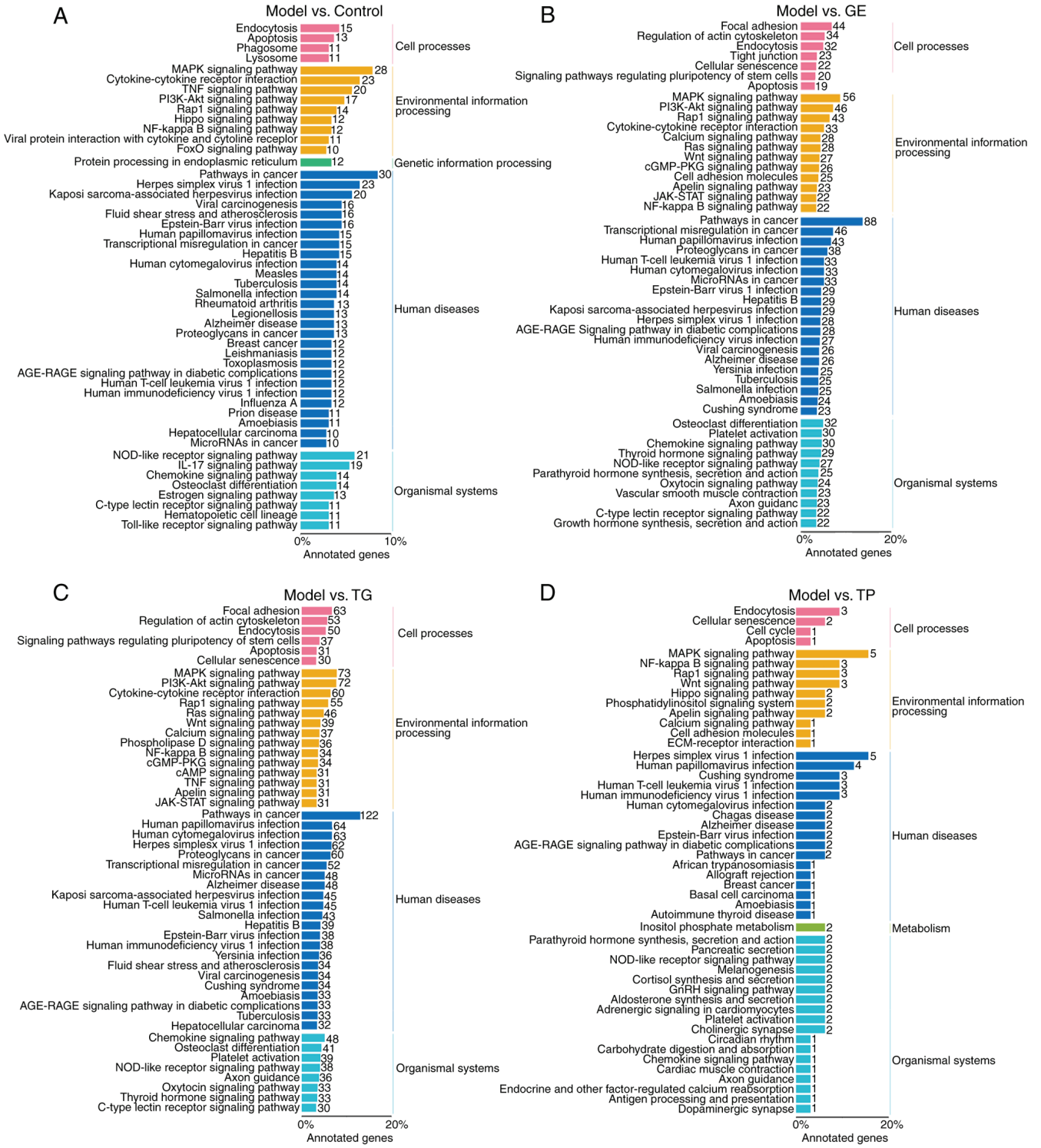

Figure 6. Top 50 KEGG pathways associated with the upregulated DEGs between the various indicated two treatment groups. KEGG classification analysis of DEGs between the (A) Model and Control groups, (B) Model and GE groups, (C) Model and TG groups and (D) Model and TP groups. DEGs, differentially expressed genes; GE, ginseng extract; KEGG, Kyoto Encyclopedia of Genes and Genomes; TG, total ginsenosides; TP, total polysaccharides.

on inhibiting cell apoptosis was significantly superior to TP (Fig. 9A). Furthermore, the expression levels of anti-apoptosis (*Bcl2* and *Mcl1*) and pro-apoptosis (*Bax*, *Bid* and *Bad*) DEGs were next analyzed. The results showed that CY significantly inhibited the expression of *Mcl1* and increased the expression of *Bax* (Fig. 9B). TG significantly increased the expression levels of *Bcl2* and *Mcl1*, whilst decreasing those of *Bax* compared with the Model group. GE significantly inhibited the expression levels of *Bax* and *Bad* compared with those in the Model and TP groups (Fig. 9B). In addition, the expression levels of *Bid* were significantly lower in the GE group compared with those in the TP group (Fig. 9B). Notably, TP had little effect on the expression levels of apoptotic genes compared with the Model group. According to the western blotting analysis, TG increased the protein expression levels of Bcl2, whereas GE and TG decreased the protein expression

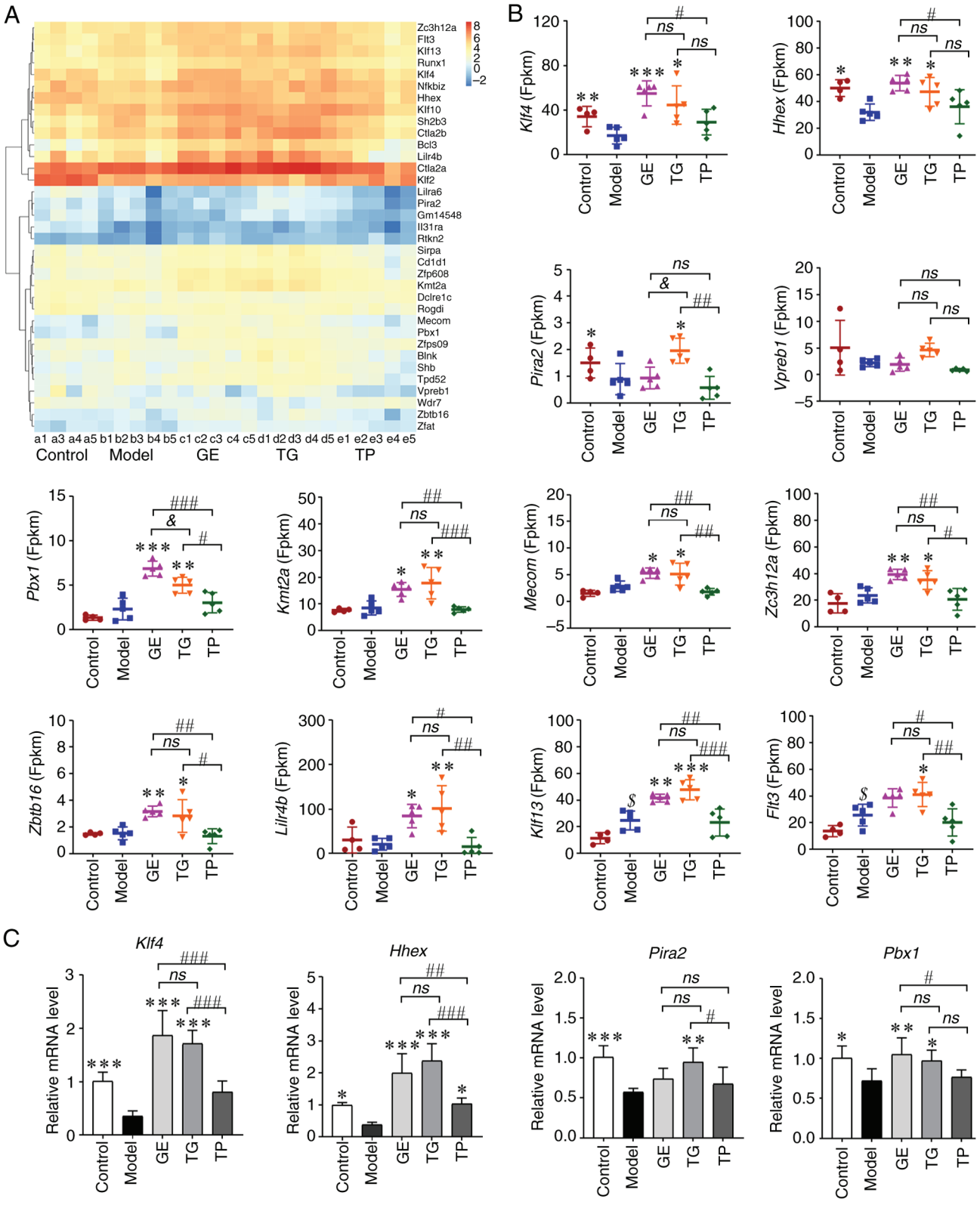

Figure 7. Expression analysis of hematopoiesis-related the upregulated DEGs in hematopoietic stem cells. (A) Heatmap of hematopoietic-related genes among samples. (B) Expression levels of hematopoiesis-related DEGs. (C) mRNA expression levels of hematopoiesis-related genes. Data are presented as the mean ± SD (n=5), *P<0.05, **P<0.01 and ***P<0.001 compared to the Model group; $^{\#}$P<0.05, $^{\#\#}$P<0.01 and $^{\#\#\#}$P<0.001; $^{\&}$P<0.05. DEGs, differentially expressed genes; GE, ginseng extract; ns, no significance; TG, total ginsenosides; TP, total polysaccharides.

levels of Bax compared with the Model group (Fig. 9C). These results suggest that both GE and TG inhibited the apoptosis of HSCs. However, the inhibitory effect of TP on cell apoptosis was weaker compared with that of GE and TG.

Effect of GE, TG and TP on the erythroid differentiation of HSCs and blood cell parameters. TER-119 has been previously used as a marker of erythroid differentiation of HSCs (38). The present study therefore detected TER-119 expression to

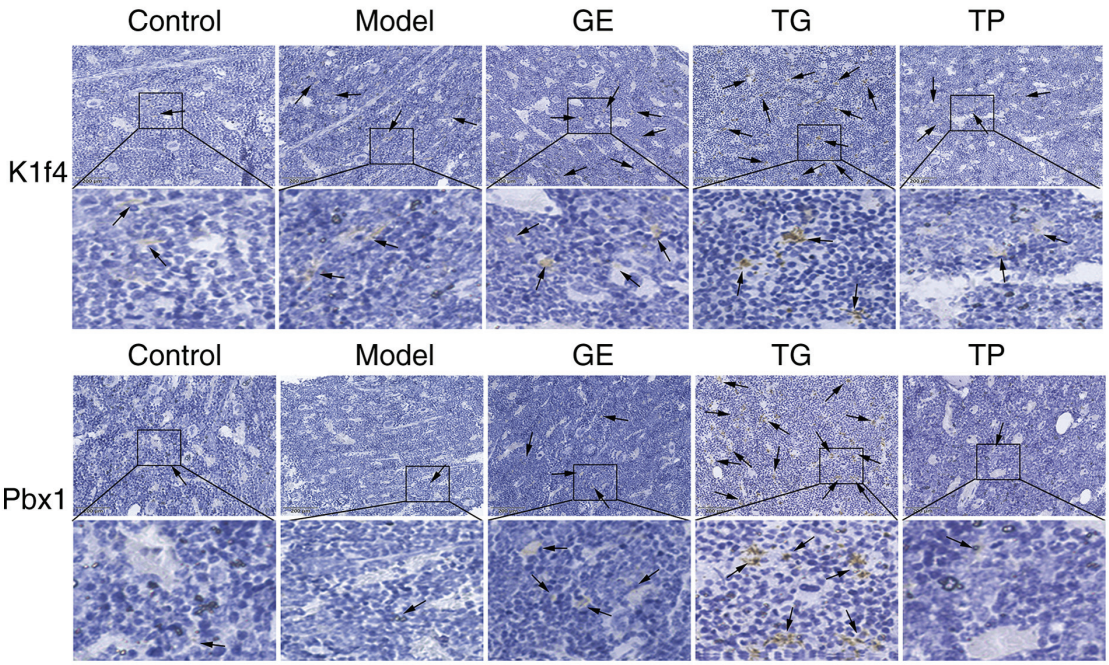

Figure 8. Protein expression of Klf4 and Pbx1 as determined by immunohistochemical staining in the mouse bone marrow (magnification, x400). (A) KLF4 and (B) pbx1 staining. The arrows show locations of positive Klf4/Pbx1 expression. GE, ginseng extract; TG, total ginsenosides; TP, total polysaccharides; KLF4, Krüppel-like factor 4.

assess the differentiation ability of HSCs induced by CY. The results showed that CY significantly reduced the expression of TER-119 compared with that in the Control group (Fig. 10A). By contrast, GE markedly increased the expression of TER-119 compared with that in the Model and TP groups (Fig. 10A). The expression of TER-119 in the TG and TP groups was not statistically different compared with that in the Model group. In the blood cell parameter analysis, the numbers of all peripheral blood cells were found to be significantly reduced in the Model mice (Fig. 10B), which were all significantly reversed by GE and TG [namely WBC, neutrophils, LYMPH, RBC, HGB, Ret and PLT; Fig. 10B]. By contrast, TP could only restore the levels of LYMPH, RBC, HGB and PLT compared with those in the Model group (Fig. 10B). TER-119 was expressed in Ret from HSCs (39), and this increasing trend in TER-119, Ret and RGB is consistent among the GE, TG, and TP groups. Notably, the improvement effect of TP on blood cells was weaker compared with that of GE and TG.

Discussion

CY is a widely used chemotherapeutic drug for the treatment of various types of cancer, such as lymphoma, breast cancer and ovarian cancer (1,2,4). CY can impair HSCs to affect the production of new blood cells, further resulting in anemia, infection and bleeding (40). In addition, CY can disrupt the balance of the intestinal microflora (7). Ginseng has previously exhibited dual efficacy in inhibiting cancer cells and protecting the immune system (29,41). Therefore, the present study assessed the effect of GE, TG and TP on the intestinal microflora and HSCs from model mice induced by CY. After drug administration for 28 days, it was revealed that GE and TG restored the phylum/genus/species levels of intestinal bacteria after CY treatment. In addition, the protective effects of GE and TG on HSCs were superior to those of TP, the latter of which was not effective at preventing CY-induced HSC damage.

The intestinal microflora regulates host metabolism and immune homeostasis, in turn maintaining the physiology of the body (18,42). The α diversity estimators revealed that CY decreased the relative abundance of some dominant microflora, whilst increasing that of some low-abundance microflora. *Lactobacillus* is a dominant and beneficial bacteria in the intestinal microflora, which has immunoregulatory effects by regulating the activity of epithelial cells, macrophages, dendritic cells and regulatory T cells (43). CY significantly decreased the relative abundance of *Lactobacillus* and *Lactobacillus_intestinalis* at the genus and species levels. American ginseng ginsenoside, cotreatment with American ginseng polysaccharide and ginsenoside have all been reported to increase the abundance of *Lactobacillus* in CY-induced mice (7). The present study showed that GE exhibited the optimal improvement at the phylum and genus levels, whereas TG showed the optimal improvement at the species level. A previous study has shown that the ginsenoside content of TG and GE is 4.39 and 81.09%, respectively, whilst the polysaccharide content of GE, TG and TP is 72.28, 4.68 and 89.79%, respectively (26). Notably, ginsenoside content was revealed to be significantly positively correlated with the abundance of *Lactobacillus_intestinalis* in the present study. Ginseng polysaccharides have been reported to change the intestinal microbiota and kynurenine/tryptophan ratio to exert anti-inflammatory and immunoregulatory effects (41,44). In the present study, TP significantly increased the abundance of low-abundance microflora, such as *Mouse_gut*, *Bacteroides_dorei*, *Prevotella_melanimogenica*, *Anaerotignum_lactatifermentans*, *Bacteroides_plebeius* and *Parabacteroides_merdae*. *Bacteroides_dorei* can reduce intestinal microbial lipopolysaccharide production (45), promote earlier IFN expression and

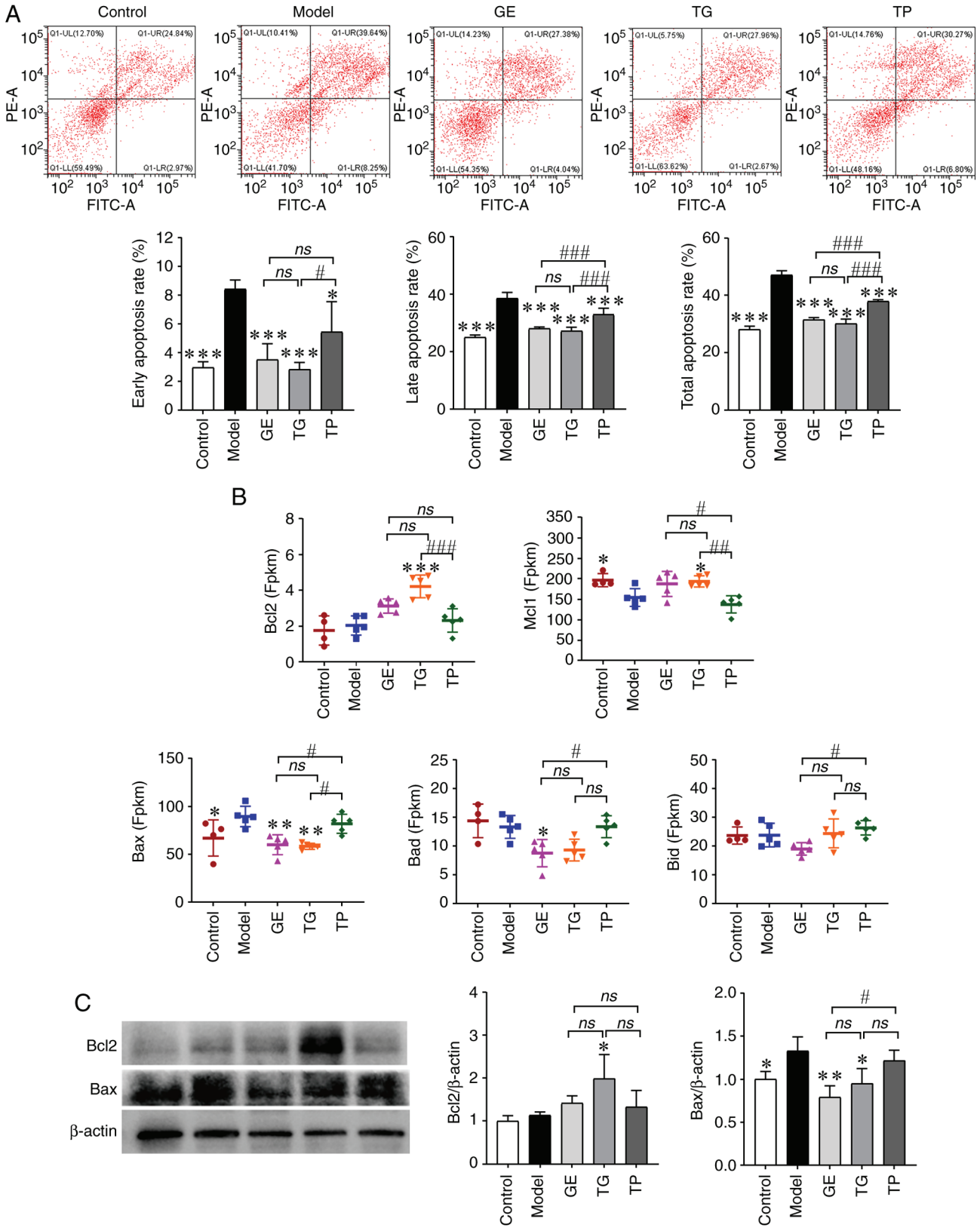

Figure 9. Effect of GE, TG and TP on the apoptosis of HSCs. (A) Apoptosis analysis of HSCs by flow cytometry. (B) Expression of apoptosis-associated genes among the differentially expressed genes. (C) Protein expression of Bcl2 and Bax. Data are presented as the mean ± SD (n=5), *P<0.05, **P<0.01 and ***P<0.001 vs. Model group; $^{\#}$P<0.05, $^{\#\#}$P<0.01 and $^{\#\#\#}$P<0.001. GE, ginseng extract; Mcl1, myeloid cell leukemia-1; HSCs, hematopoietic stem cells; ns, no significance; TG, total ginsenosides; TP, total polysaccharides.

inhibit both local and systemic inflammatory responses (46). Park *et al* (47) previously reported that *Bacteroides_plebeius* contains an endo-type β-agarase, BpGH16A, which is the key enzyme that initiates the depolymerization of agarose, where supplementary *Bacteroides_plebeius* can recover disturbances of the intestinal microbiota in chronic kidney

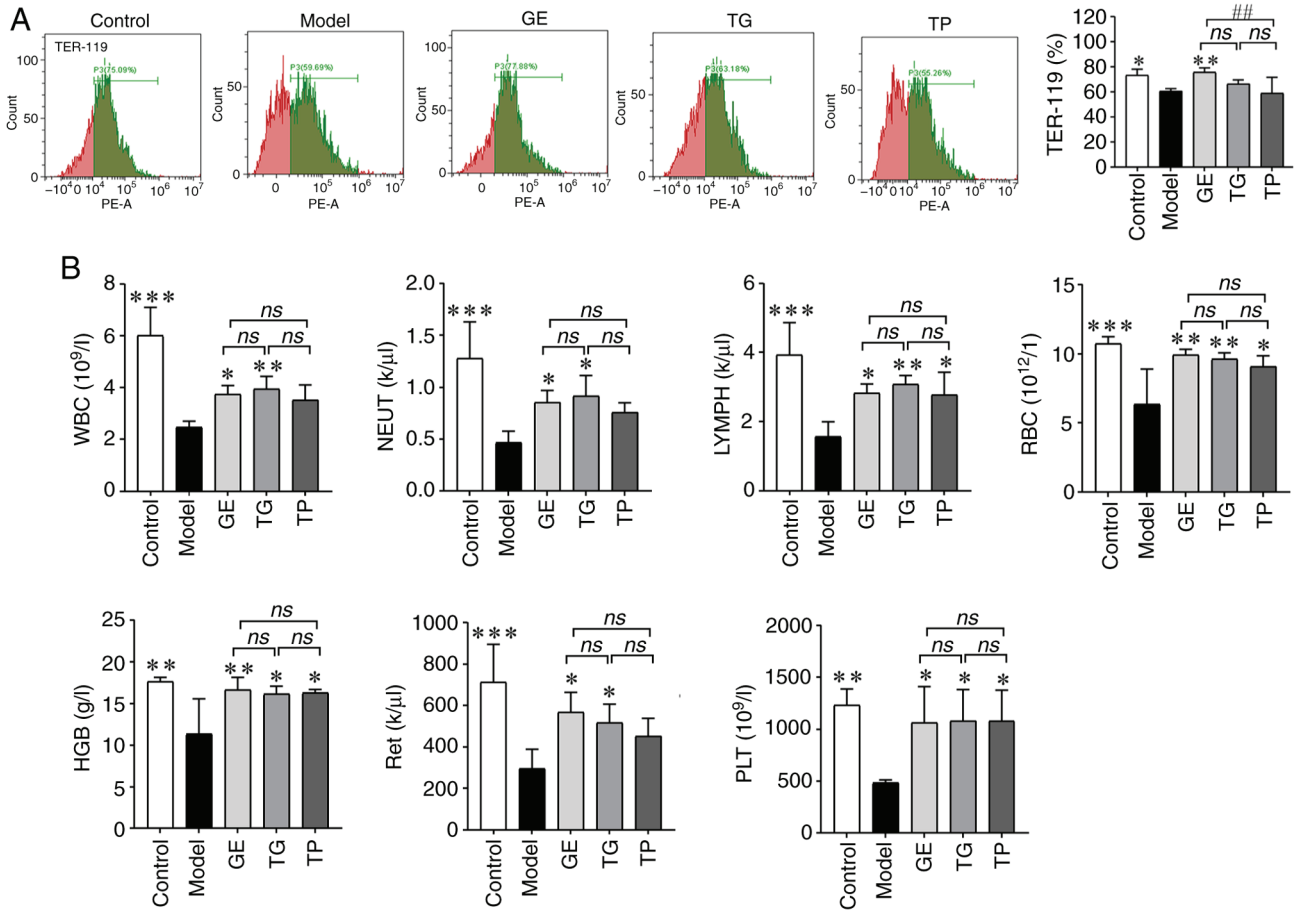

Figure 10. Effect of GE, TG and TP on the erythroid differentiation of hematopoietic stem cells and blood cell parameters. (A) Expression of TER-119 detected by flow cytometry. (B) Effect of GE, TG and TP on blood cell parameters. Data are presented as the mean ± SD (n=5). *P<0.05, **P<0.01 and ***P<0.001 vs. Model group; $^{\#\#}$P<0.01. GE, ginseng extract; HGB, hemoglobin; LYMPH, lymphocyte; NEUT, neutrophil; ns, no significance; PLT, platelet; RBC, red blood cell; Ret, reticulocyte; TG, total ginsenosides; TP, total polysaccharides; WBC, white blood cell.

disease (48). *Prevotella_melanimogenica* has been associated with infections in humans (49), where an increase in the abundance of *Prevotella* can improve glucose metabolism (50). *Parabacteroides_merdae* has been shown to promote branched-chain amino acid catabolism to alleviate obesity and hyperlipidemia (51). Therefore, TP likely participates in the process of immune regulation and inflammation by regulating the intestinal microflora of model mice induced by CY. The aforementioned results indicated that GE, TG and TP can all alleviate CY-induced abnormalities in intestinal microbiota. However, the species of intestinal bacteria altered by TP was different from those altered by GE and TG.

CY can induce the apoptosis of HSCs to reduce the number of blood cells (6). In the high-throughput RNA-seq analysis, CY was found to markedly inhibit the expression levels of genes associated with hematopoietic function (such as *Hhex*, *Klf4* and *Pira2*) of the bone marrow, whilst increasing those of *Flt3* (52) and *Klf13*. The total extract from Korean red ginseng mainly includes ginsenoside Rg1, ginsenoside Re, ginsenoside Rf, ginsenoside Rg2, ginsenoside Rb1, ginsenoside Rb2, ginsenoside Rc and ginsenoside Rd, which can promote $CD34^{+}$ cell expansion and hematopoietic colony formation, especially those of the erythroid lineage (53). Ginsenoside Rg1 exerts protective effects on HSCs by improving redox homeostasis. Cao *et al* (35) previously reported that ginsenoside Rg1 can reduce reactive oxygen species levels, increase the number of mitochondria and the ratio of Bcl2/Bax, which recovered hematopoietic function by inhibiting Bax translocation-mediated mitochondrial apoptosis in aplastic anemia mice. Ginsenoside Rd has been reported to promote human induced pluripotent stem cell differentiation into myoblasts through the Flt3 signaling pathway (54). Flt3 can prevent stem cells and progenitors from spontaneous apoptotic cell death by upregulating Mcl1, which is an indispensable survival factor of hematopoiesis (55). CK has been shown to promote cell cycle entry in bone marrow nucleated cells through the Bcl2/Bax and MEK/ERK signaling pathways, which can also increase peripheral blood cells of myelosuppression mice induced by CY (56).

In the present study, the DEGs in the GE and TG groups were mainly enriched in HSCs-related signaling pathways, such as PI3K/Akt signaling pathway, Rap1 signaling pathway, cytokine-cytokine receptor interaction, Ras signaling pathway, Wnt signaling pathway, TNF signaling pathway, apelin signaling pathway, JAK-STAT signaling pathway and NF-κB signaling pathway (36,37). Tang *et al* (57) reported that Rg1 delayed hematopoietic stem/progenitor cell senescence by increasing protein expression of SIRT6, inhibiting protein expression of NF-κB and overactivation of the Wnt/β-catenin through regulating the SIRT6/NF-κB signaling pathway and Wnt/β-catenin signaling pathway. Certain genes identified in

the present study, such as *Klf4*, *Hhex*, *Pira2*, *Pbx1*, *Kmt2a*, *Mecom*, *Zc3h12a*, *Zbtb16*, *Lilr4b*, *Flt3* and *Klf13*, are involved in the self-renewal and differentiation of HSCs (55,58-63), TG markedly increased the expression levels of the aforementioned genes. GE significantly enhanced the levels of *Hhex*, *Klf4*, *Pbx1*, *Kmt2a*, *Mecom*, *Zc3h12a*, *Zbtb16*, *Lilr4b*, *Flt3* and *Klf13*, but TP barely increased the expression of these genes. TG exerted the optimal protective effect on HSCs, followed by GE and then TP, the latter of which was not effective.

TP is mainly composed of macromolecular polysaccharide components, which have difficulty directly acting on target organs to improve tissue damage (64). However, TP has been reported to ameliorate intestinal immune disorders and inflammation by improving the intestinal microbiota (7). A previous study has demonstrated that 12 ginsenosides are present in GE and TG, including nR1, Rg1, Re, Rf, Ra2, Rb1, Rc, Ro, Rb2, Rb3, Rd and 20(R)-Rg3 (6). Therefore, it may be hypothesized that the content of ginsenosides is positively associated with the upregulated gene expression in HSCs. However, GE, TG and TP were extracted by our laboratory and there is currently no standard protocol for extraction, which is a limitation of the present study. Chen *et al* (29) reported that GE enhanced the immune regulation and antioxidant levels of immunosuppressed mice caused by CY. In another study, Tang *et al* (65) revealed that the purity of TG was 90-93% by heating and refluxing with petroleum ether and water-saturated n-butanol solution, which then alleviated the CY-induced liver injury of mice by regulating the imbalance of intestinal microflora. Furthermore, TG (purity >70%) from the stem and leaf of *Panax ginseng* has been shown to inhibit the apoptosis and genotoxicity of bone marrow and peripheral lymphocyte cells induced by CY (5). In addition, TP (purity >90%) may promote natural killer cell cytotoxicity in immunosuppressed mice (66). Wan *et al* (23) reported that TP, which was extracted sequentially by 95% ethanol, hot water and 95% ethanol, modulated tryptophan metabolism by improving the gut microbiota, which resulted in the amelioration of impaired intestinal barrier and the alleviation of the inflammatory microenvironment formation of ulcerative colitis mice induced by dextran sulfate sodium. Differential extraction methods will likely lead to differences in the chemical composition of GE, TG and TP. However, different components from ginseng can improve the damage caused by CY.

Ginsenosides have low oral bioavailability and absorption in the body. Zhou *et al* (67) reported that ginseng polysaccharides can promote the exposure and absorption of ginsenosides. Li *et al* (68) studied the synergistic effects of TP and ginsenoside Rb1, before finding that the presence of TP accelerated the microbial metabolism of Rb1 and promoted fecal β-D-glucosidase activity, which then transformed into Rd and CK. In particular, the biotransformation rate of CK was increased from 14.0 to 86.7%. Furthermore, TP can promote Rb1 transport across a Caco-2 cell monolayer (15). Wang *et al* (69) also found that polysaccharides promoted the metabolism of ginsenosides. In the present study, GE and TG protected HSCs from damage induced by CY.

In the present study, animal models provided valuable mechanistic insights. Namely, GE and TG were suggested to activate the expression of HSC related-genes and proteins to inhibit the apoptosis of HSCs of normal (non-tumorous) mice induced by CY. However, their translation into a clinical setting has specific challenges. HSC and progenitor cell self-renewal and differentiation are complex processes that are important for the production and long-term maintenance of all cell lineages and blood cells (70). However, HSCs and progenitor cells also directly and indirectly participate in both tumor immune escape and the metastatic cascade (71,72). In the future, research on mouse models of different types of cancer is required to confirm the protective effect of ginsenosides on HSCs.

In conclusion, CY can damage HSCs, which can cause intestinal microflora disorder and cell apoptosis, inhibit the differentiation of HSCs and reduce the number of peripheral blood cells. The present results showed that GE and TG can effectively improve the imbalance of intestinal microflora and protect HSCs from damage induced by CY. GE and TG inhibited the disordered gut microbiota. Specifically, the relative abundances of *Lactobacillus* and *Lactobacillus_intestinalis* were higher in the GE and TG groups compared with those in the Model group. However, TP mainly increased the abundance of beneficial microflora with low-abundance. Furthermore, GE and TG could activate the expression of hematopoietic-related genes by mediating multiple signaling pathways of HSCs. GE blocked the apoptosis of HSCs by inhibiting the expression of Bax and Bad, whereas TG prevented the apoptosis of HSCs by promoting the expression of Bcl2 and Mcl1 and inhibiting the expression of Bax. Notably, GE is similar to TG, it exhibited a protective effect on a mouse model of HSC damage induced by CY. These findings suggest that ginsenosides can prevent or alleviate HSC damage.

Acknowledgements

Not applicable.

Funding

The present study was supported by the Science and Technology Development Plan Project of Jilin Province (grant no. YDZJ202401417ZYTS), the Science and Technology Major Project of Jilin Province (grant no. 20210304001YY), the Science and Technology Projects of Education Department of Jilin Province (grant nos. JJKH20230990KJ and JJKH20230976KJ), the Cultivation Project of Young Discipline Backbone Talent (grant no. 202320) and the Innovation and Entrepreneurship Talent Funding Project of Jilin Province (grant no. 2022ZY10).

Availability of data and materials

The 16S rRNA sequencing data generated in the present study may be found in the BioProject database under accession number PRJNA934302 or at the following URL: https://www.ncbi.nlm.nih.gov/bioproject/?term=PRJNA934302. The other data generated in the present study may be requested from the corresponding author.

Authors' contributions

ZL, XG, DZ, XL, HS and HZ contributed to the study conception and design. ZL, TY, CJ, XG, WQ and LZ contributed to

project development and data collection. ZL, TY, XG and CJ contributed to protocol development and manuscript writing. XG, LZ, YY and JO contributed to data collection and analysis. HS and HZ contributed to data analysis and manuscript editing. ZL, XG and HZ confirm the authenticity of all the raw data. All authors read and approved the final version of the manuscript.

Ethics approval and consent to participate

All animal experiments were approved and performed by the Ethics Committee of Changchun University of Chinese Medicine (Changchun, China; approval no. 2023033).

Patient consent for publication

Not applicable.

Competing interests

The authors declare that they have no competing interests.

References

1. Burke JM, Masaquel A, Wang R, Hossain F, Li J, Zhou SQ, Ng CD and Matasar M: Cost of disease progression in diffuse large B-cell lymphoma after frontline treatment with rituximab plus cyclophosphamide, doxorubicin, vincristine, and prednisone. Clin Lymphoma Myeloma Leuk 23: e393-e404, 2023.
2. Velikova G, Morden JP, Haviland JS, Emery C, Barrett-Lee P, Earl H, Bloomfield D, Brunt AM, Canney P, Coleman R, *et al*: Accelerated versus standard epirubicin followed by cyclophosphamide, methotrexate, and fluorouracil or capecitabine as adjuvant therapy for breast cancer (UK TACT2; CRUK/05/19): Quality of life results from a multicentre, phase 3, open-label, randomised, controlled trial. Lancet Oncol 24: 1359-1374, 2023.
3. Chen Y, Ai L, Zhang Y, Li X, Xu S, Yang W, Jin J, Ma Y, Hu Z, Zhang Y, *et al*: The EZH2-H3K27me3 axis modulates aberrant transcription and apoptosis in cyclophosphamide-induced ovarian granulosa cell injury. Cell Death Discov 9: 413, 2023.
4. Kang H, Fan W, Lei B, Tian Y and Zhang S: The immunosuppression and immunoenhancement effects of cyclophosphamide on normal mice. Immunol J 34: 308-312, 2018.
5. Zhang QH, Wu CF, Duan L and Yang JY: Protective effects of total saponins from stem and leaf of *Panax ginseng* against cyclophosphamide-induced genotoxicity and apoptosis in mouse bone marrow cells and peripheral lymphocyte cells. Food Chem Toxicol 46: 293-302, 2008.
6. Zhang H, Sun Y, Fan M, Zhang Y, Liang Z, Zhang L, Gao X, He X, Li X, Zhao D, *et al*: Prevention effect of total ginsenosides and ginseng extract from *Panax ginseng* on cyclophosphamide-induced immunosuppression in mice. Phytother Res 37: 3583-3601, 2023.
7. Zhou R, He D, Xie J, Zhou Q, Zeng H, Li H and Huang L: The synergistic effects of polysaccharides and ginsenosides from American ginseng (*Panax quinquefolius* L.) ameliorating cyclophosphamide-induced intestinal immune disorders and gut barrier dysfunctions based on microbiome-metabolomics analysis. Front Immunol 12: 665901, 2021.
8. Viaud S, Saccheri F, Mignot G, Yamazaki T, Daillère R, Hannani D, Enot DP, Pfirschke C, Engblom C, Pittet MJ, *et al*: The intestinal microbiota modulates the anticancer immune effects of cyclophosphamide. Science 342: 971-976, 2013.
9. Qi L, Wang C and Yuan C: Ginsenosides from American ginseng: Chemical and pharmacological diversity. Phytochemistry 72: 689-699, 2011.
10. Qu D, Huo XH, Li ZM, Hua M, Lu YS, Chen JB, Li SS, Wen LK and Sun YS: Sediment formation and analysis of the main chemical components of aqueous extracts from different parts of ginseng roots. Food Chem 379: 132146, 2022.
11. Yance DR Jr and Sagar SM: Targeting angiogenesis with integrative cancer therapies. Integr Cancer Ther 5: 9-29, 2006.
12. Wan Y, Wang J, Xu JF, Tang F, Chen L, Tan YZ, Rao CL, Ao H and Peng C: *Panax ginseng* and its ginsenosides: potential candidates for the prevention and treatment of chemotherapy-induced side effects. J Ginseng Res 45: 617-630, 2021.
13. Jia L, Zhao Y and Liang XJ: Current evaluation of the millennium phytomedicine-ginseng (II): Collected chemical entities, modern pharmacology, and clinical applications emanated from traditional Chinese medicine. Curr Med Chem 16: 2924-2942, 2009.
14. Cockburn DW and Koropatkin NM: Polysaccharide degradation by the intestinal microbiota and its influence on human health and disease. J Mol Biol 428: 3230-3252, 2016.
15. Shen H, Gao XJ, Li T, Jing WH, Han BL, Jia YM, Hu N, Yan ZX, Li SL and Yan R: Ginseng polysaccharides enhanced ginsenoside Rb1 and microbial metabolites exposure through enhancing intestinal absorption and affecting gut microbial metabolism. J Ethnopharmacol 216: 47-56, 2018.
16. Maiuolo J, Musolino V, Gliozzi M, Carresi C, Scarano F, Nucera S, Scicchitano M, Oppedisano F, Bosco F, Macri R, *et al*: Involvement of the intestinal microbiota in the appearance of multiple sclerosis: Aloe vera and citrus bergamia as potential candidates for intestinal health. Nutrients 14: 2711, 2022.
17. Li S, Han W, He Q, Zhang W and Zhang Y: Relationship between intestinal microflora and hepatocellular cancer based on gut-liver axis theory. Contrast Media Mol Imaging 2022: 6533628, 2022.
18. Marchesi JR, Adams DH, Fava F, Hermes GD, Hirschfield GM, Hold G, Quraishi MN, Kinross J, Smidt H, Tuohy KM, *et al*: The gut microbiota and host health: A new clinical frontier. Gut 65: 330-339, 2016.
19. Yang Z and Ji G: *Fusobacterium* nucleatum-positive colorectal cancer. Oncol Lett 18: 975-982, 2019.
20. Kostic AD, Gevers D, Pedamallu CS, Michaud M, Duke F, Earl AM, Ojesina AI, Jung J, Bass AJ, Tabernero J, *et al*: Genomic analysis identifies association of *Fusobacterium* with colorectal carcinoma. Genome Res 22: 292-298, 2012.
21. Kim YK and Yum KS: Effects of red ginseng extract on gut microbial distribution. J Ginseng Res 46: 91-103, 2022.
22. Ding Q, Feng SW, Xu GH, Chen YY and Shi YY: Effects of total ginsenosides from *Panax ginseng* stems and leaves on gut microbiota and short-chain fatty acids metabolism in acute lung injury mice. Zhongguo Zhong Yao Za Zhi 48: 1319-1329, 2023 (In Chinese).
23. Wan L, Qian C, Yang C, Peng S, Dong G, Cheng P, Zong G, Han H, Shao M, Gong G, *et al*: Ginseng polysaccharides ameliorate ulcerative colitis via regulating gut microbiota and tryptophan metabolism. Int J Biol Macromol 265: 130822, 2024.
24. Mazur L, Augustynek A, Deptała A, Halicka HD and Bedner E: Effects of WR-2721 and cyclophosphamide on the cell cycle phase specificity of apoptosis in mouse bone marrow. Anticancer Drugs 13: 751-758, 2002.
25. Wang JB, Du MW and Zheng Y: Effect of ginsenoside Rg1 on hematopoietic stem cells in treating aplastic anemia in mice via MAPK pathway. World J Stem Cells 16: 591-603, 2024.
26. Zhang Y, Zhang L, Zhou W, Zhang X, Su W, Wei X and Zhang H: Protective effect of various types of ginseng extracts on blood deficiency induced by cyclophosphamide in rat. Lishizhen Med Mater Med Res 33: 2861-2867, 2022 (In Chinese).
27. Duan Y, Huang J, Sun M, Jiang Y, Wang S, Wang L, Yu N, Peng D, Wang Y, Chen W and Zhang Y: Poria cocos polysaccharide improves intestinal barrier function and maintains intestinal homeostasis in mice. Int J Biol Macromol 249: 125953, 2023.
28. Boonlert W, Benya-Aphikul H, Umka Welbat J and Rodsiri R: Ginseng extract G115 attenuates ethanol-induced depression in mice by increasing brain BDNF levels. Nutrients 9: 931, 2017.
29. Chen LX, Qi YL, Qi Z, Gao K, Gong RZ, Shao ZJ, Liu SX, Li SS and Sun YS: A comparative study on the effects of different parts of *Panax ginseng* on the immune activity of cyclophosphamide-induced immunosuppressed mice. Molecules 24: 1096, 2019.
30. Parasuraman S, Raveendran R and Kesavan R: Blood sample collection in small laboratory animals. J Pharmacol Pharmacother 1: 87-93, 2010.
31. Zhao H, Lyu Y, Zhai R, Sun G and Ding X: Metformin mitigates sepsis-related neuroinflammation via modulating gut microbiota and metabolites. Front Immunol 13: 797312, 2022.
32. Young MD, Wakefield MJ, Smyth GK and Oshlack A: Gene ontology analysis for RNA-seq: Accounting for selection bias. Genome Biol 11: R14, 2010.

33. Mao X, Cai T, Olyarchuk JG and Wei L: Automated genome annotation and pathway identification using the KEGG Orthology (KO) as a controlled vocabulary. Bioinformatics 21: 3787-3793, 2005.
34. Livak KJ and Schmittgen TD: Analysis of relative gene expression data using real-time quantitative PCR and the 2(-Delta Delta C(T)) method. Methods 25: 402-408, 2001.
35. Cao H, Wei W, Xu R and Cui X: Ginsenoside Rg1 can restore hematopoietic function by inhibiting Bax translocation-mediated mitochondrial apoptosis in aplastic anemia. Sci Rep 11: 12742, 2021.
36. de Roo JJD and Staal FJT: Cell signaling pathway reporters in adult hematopoietic stem cells. Cells 9: 2264, 2020.
37. Montazersaheb S, Ehsani A, Fathi E and Farahzadi R: Cellular and molecular mechanisms involved in hematopoietic stem cell aging as a clinical prospect. Oxid Med Cell Longev 2022: 2713483, 2022.
38. An X and Chen L: Flow cytometry (FCM) analysis and fluorescence-activated cell sorting (FACS) of erythroid cells. Methods Mol Biol 1698: 153-174, 2018.
39. Asari S, Sakamoto A, Okada S, Ohkubo Y, Arima M, Hatano M, Kuroda Y and Tokuhisa T: Abnormal erythroid differentiation in neonatal bcl-6-deficient mice. Exp Hematol 33: 26-34, 2005.
40. Kurtin S: Myeloid toxicity of cancer treatment. J Adv Pract Oncol 3: 209-224, 2012.
41. Huang J, Liu D, Wang Y, Liu L, Li J, Yuan J, Jiang Z, Jiang Z, Hsiao WW, Liu H, *et al*: Ginseng polysaccharides alter the gut microbiota and kynurenine/tryptophan ratio, potentiating the antitumour effect of antiprogrammed cell death 1/programmed cell death ligand 1 (anti-PD-1/PD-L1) immunotherapy. Gut 71: 734-745, 2022.
42. O'Hara AM, O'Regan P, Fanning A, O'Mahony C, Macsharry J, Lyons A, Bienenstock J, O'Mahony L and Shanahan F: Functional modulation of human intestinal epithelial cell responses by Bifidobacterium infantis and *Lactobacillus* salivarius. Immunology 118: 202-215, 2006.
43. Christensen HR, Frøkiaer H and Pestka JJ: Lactobacilli differentially modulate expression of cytokines and maturation surface markers in murine dendritic cells. J Immunol 168: 171-178, 2002.
44. Li S, Huo X, Qi Y, Ren D, Li Z, Qu D and Sun Y: The protective effects of Ginseng polysaccharides and their effective subfraction against dextran sodium sulfate-induced colitis. Foods 11: 980, 2022.
45. Yoshida N, Emoto T, Yamashita T, Watanabe H, Hayashi T, Tabata T, Hoshi N, Hatano N, Ozawa G, Sasaki N, *et al*: *Bacteroides* vulgatus and *Bacteroides* dorei reduce gut microbial lipopolysaccharide production and inhibit atherosclerosis. Circulation 138: 2486-2498, 2018.
46. Song L, Huang Y, Liu G, Li X, Xiao Y, Liu C, Zhang Y, Li J, Xu J, Lu S and Ren Z: A novel immunobiotics *Bacteroides* dorei ameliorates influenza virus infection in mice. Front Immunol 12: 828887, 2022.
47. Park NJ, Yu S, Kim DH, Yun EJ and Kim KH: Characterization of BpGH16A of *Bacteroides* plebeius, a key enzyme initiating the depolymerization of agarose in the human gut. Appl Microbiol Biotechnol 105: 617-625, 2021.
48. Pei T, Zhu D, Yang S, Hu R, Wang F, Zhang J, Yan S, Ju L, He Z, Han Z, *et al*: *Bacteroides* plebeius improves muscle wasting in chronic kidney disease by modulating the gut-renal muscle axis. J Cell Mol Med 26: 6066-6078, 2022.
49. Tett A, Pasolli E, Masetti G, Ercolini D and Segata N: *Prevotella* diversity, niches and interactions with the human host. Nat Rev Microbiol 19: 585-599, 2021.
50. Kovatcheva-Datchary P, Nilsson A, Akrami R, Lee YS, De Vadder F, Arora T, Hallen A, Martens E, Björck I and Bäckhed F: Dietary fiber-induced improvement in glucose metabolism is associated with increased abundance of *Prevotella*. Cell Metab 22: 971-982, 2015.
51. Qiao S, Liu C, Sun L, Wang T, Dai H, Wang K, Bao L, Li H, Wang W, Liu SJ and Liu H: Gut *Parabacteroides* merdae protects against cardiovascular damage by enhancing branched-chain amino acid catabolism. Nat Metab 4: 1271-1286, 2022.
52. El-Serafi I, Abedi-Valugerdi M, Potácová Z, Afsharian P, Mattsson J, Moshfegh A and Hassan M: Cyclophosphamide alters the gene expression profile in patients treated with high doses prior to stem cell transplantation. PLoS One 9: e86619, 2014.
53. Kim SG, Lee AJ, Bae SH, Kim SM, Lee JH, Kim MJ and Jang HB: Total extract of Korean red ginseng facilitates human bone marrow hematopoietic colony formation in vitro. Blood Res 49: 177-181, 2014.
54. Sun C, Choi IY, Rovira Gonzalez YI, Andersen P, Talbot CC Jr, Iyer SR, Lovering RM, Wagner KR and Lee G: Duchenne muscular dystrophy hiPSC-derived myoblast drug screen identifies compounds that ameliorate disease in mdx mice. JCI Insight 5: e134287, 2020.
55. Kikushige Y, Yoshimoto G, Miyamoto T, Iino T, Mori Y, Iwasaki H, Niiro H, Takenaka K, Nagafuji K, Harada M, *et al*: Human Flt3 is expressed at the hematopoietic stem cell and the granulocyte/macrophage progenitor stages to maintain cell survival. J Immunol 180: 7358-7367, 2008.
56. Han J, Wang Y, Cai E, Zhang L, Zhao Y, Sun N, Zheng X and Wang S: Study of the effects and mechanisms of ginsenoside compound K on myelosuppression. J Agric Food Chem 67: 1402-1408, 2019.
57. Tang YL, Zhou Y, Wang YP, Wang JW and Ding JC: SIRT6/NF-κB signaling axis in ginsenoside Rg1-delayed hematopoietic stem/progenitor cell senescence. Int J Clin Exp Pathol 8: 5591-5596, 2015.
58. Jackson JT, O'Donnell K, Light A, Goh W, Huntington ND, Tarlinton DM and McCormack MP: Hhex regulates murine lymphoid progenitor survival independently of Stat5 and Cdkn2a. Eur J Immunol 50: 959-971, 2020.
59. Klaewsongkram J, Yang Y, Golech S, Katz J, Kaestner KH and Weng NP: Krüppel-like factor 4 regulates B cell number and activation-induced B cell proliferation. J Immunol 179: 4679-4684, 2007.
60. Feinberg MW, Wara AK, Cao Z, Lebedeva MA, Rosenbauer F, Iwasaki H, Hirai H, Katz JP, Haspel RL, Gray S, *et al*: The Kruppel-like factor KLF4 is a critical regulator of monocyte differentiation. EMBO J 26: 4138-4148, 2007.
61. Ficara F, Murphy MJ, Lin M and Cleary ML: Pbx1 regulates self-renewal of long-term hematopoietic stem cells by maintaining their quiescence. Cell Stem Cell 2: 484-496, 2008.
62. Voit RA and Sankaran VG: MECOM deficiency: From bone marrow failure to impaired B-cell development. J Clin Immunol 43: 1052-1066, 2023.
63. Matsushita K, Takeuchi O, Standley DM, Kumagai Y, Kawagoe T, Miyake T, Satoh T, Kato H, Tsujimura T, Nakamura H and Akira S: Zc3h12a is an RNase essential for controlling immune responses by regulating mRNA decay. Nature 458: 1185-1190, 2009.
64. Wang X, Luo Y, Xiu W, Xu M and Ma Y: Preparation and evaluation of sweet corn cob polysaccharide nano emulsion. Sci Tech Food Ind 43: 124-133, 2022.
65. Tang P, Ren G, Zou H, Liu S, Zhang J, Ai Z, Hu Y, Cui L, Nan B, Zhang Z and Wang Y: Ameliorative effect of total ginsenosides from heat-treated fresh ginseng against cyclophosphamide-induced liver injury in mice. Curr Res Food Sci 8: 100734, 2024.
66. Sun Y, Guo M, Feng Y, Zheng H, Lei P, Ma X, Han X, Guan H and Hou D: Effect of ginseng polysaccharides on NK cell cytotoxicity in immunosuppressed mice. Exp Ther Med 12: 3773-3777, 2016.
67. Zhou S, Xu J, Zhu H, Wu J, Xu JD, Yan R, Li XY, Liu HH, Duan SM, Wang Z, *et al*: Gut microbiota-involved mechanisms in enhancing systemic exposure of ginsenosides by coexisting polysaccharides in ginseng decoction. Sci Rep 6: 22474, 2016.
68. Li J, Li R, Li N, Zheng F, Dai Y, Ge Y, Yue H and Yu S: Mechanism of antidiabetic and synergistic effects of ginseng polysaccharide and ginsenoside Rb1 on diabetic rat model. J Pharm Biomed Anal 158: 451-460, 2018.
69. Wang HY, Wang C, Guo SC, Chen ZC, Peng ZT, Duan R, Dong TTX and Tsim KWK: Polysaccharide deriving from Ophiopogonis Radix promotes metabolism of ginsenosides in the present of human gut microbiota based on UPLC-MS/MS assay. J Pharm Biomed Anal 175: 112779, 2019.
70. Gbyli R, Song Y and Halene S: Humanized mice as preclinical models for myeloid malignancies. Biochem Pharmacol 174: 113794, 2020.
71. Cackowski FC and Taichman RS: Parallels between hematopoietic stem cell and prostate cancer disseminated tumor cell regulation. Bone 119: 82-86, 2019.
72. Steenbrugge J, De Jaeghere EA, Meyer E, Denys H and De Wever O: Splenic hematopoietic and stromal cells in cancer progression. Cancer Res 81: 27-34, 2021.